CHALMERS
UNIVERSITY OF TECHNOLOGY

Urban Mesh Networking with LoRa

A Feasibility Study of Ground-Level Sensor Mesh Networks using LoRa Protocol for Internet of Things Applications

Master's thesis in Master of Communications Engineering

Karam Akar and Erik Higbie

Department of Electrical Engineering
CHALMERS UNIVERSITY OF TECHNOLOGY
Gothenburg, Sweden 2021

Master's thesis 2021:2

Urban Mesh Networking with LoRa

A Feasibility Study of Ground-Level Sensor Mesh Networks using LoRa Protocol for Internet of Things Applications

Karam Akar and Erik Higbie

CHALMERS
UNIVERSITY OF TECHNOLOGY

Department of Electrical Engineering
Division of Communications, Antennas, and Optical Networks
Communication Systems Group
Chalmers University of Technology
Gothenburg, Sweden 2021

Urban Mesh Networking with LoRa
A Feasibility Study of Ground-Level Sensor Mesh Networks using LoRa Protocol for Internet of Things Applications
Karam Akar and Erik Higbie

Supervisor: Mohammed Farsi, Department of Electrical Engineering
Examiner: Tommy Svensson, Department of Electrical Engineering

Master's Thesis 2021:2
Department of Electrical Engineering
Division of Communications, Antennas, and Optical Networks
Communications Systems Group
Chalmers University of Technology
SE-412 96 Gothenburg
Telephone +46 31 772 1000

Cover: Heatmap of wireless connectivity at 869.4 MHz in downtown Gothenburg constructed in Matlab.

Typeset in LaTeX
Printed by Teknologtryck
Gothenburg, Sweden 2021

Urban Mesh Networking with LoRa
A Feasibility Study of Ground-Level Sensor Mesh Networks using LoRa Protocol for Internet of Things Applications
Karam Akar and Erik Higbie
Department of Electrical Engineering
Chalmers University of Technology

Abstract

Advancements in the sensor networking field, both software and hardware, while utilizing low-cost embedded devices, has helped outline the Internet of Things (IoT) framework and slowly bring it from aspirations into reality. Wireless sensor networks can be adopted in private, small-sized projects like workplace monitoring, threat detection or resource allocation. Being also scalable to intra-city projects where a city can have its different infrastructure units like water, sanitation, transportation, agriculture, healthcare, etc., linked through sub-networks and connected through a backhaul to the main network core, making wireless sensor networking technology become a buzz word in Information and communication technology field.
Thus, this thesis undertakes hurdles that still exist when it comes to wireless sensor outdoor deployments, specifically in urban environments on the ground-level, due to the harshness of the wireless channel effects on signal propagation and the hardware restrictions imposed by the embedded devices.
Pycom embedded devices were used, called 'LoPy', that utilize LoRa (Low power, long-range) communication technology to link the different modules to test the viability of an outdoor ground-level deployment of wireless sensor networks in a confined location in central Gothenburg. The study argues for the benefit of adopting this set-up in a decentralized mesh architecture approach for the network as opposed to star topology used by LoRaWAN to provide better connectivity range in the extreme urban RF environment by utilizing mesh properties like node hopping and redundancy.
Along with the creation of a prototype sensor network and empirical testing of the Quality of Service (QoS) metrics for such network deployments, the report also provides an attempt at creating a path loss model to predict the connectivity status of the nodes in the network by tracking several quantitative assessment measures like packet success rate and RSSI with respect to the location of the nodes to assess the correctness of the model and the feasibility of the demonstration created.

Keywords: Internet of things (IoT), Wireless Sensor Networks (WSN), Quality of Service (Qos), mesh, shadowing, attenuation, urban.

Acknowledgements

We would like to express our deepest appreciation first and foremost to our Examiner, Professor Tommy Svensson at Chalmers, who provided us with not only a great deal of academic advisory and guidance, but also for his continuous and relentless moral support and encouragement to be the best version of ourselves throughout the course of the thesis. Many thanks are due and extended to the entirety of the staff at Infotiv, especially our supervisors there, Hugo Frost, Nils Gangby, Niels Jonsson, and Olle Norelius for not only their hospitality but also their support in every way they were able to offer whether in terms of resources, supervision, consultation, and the time and space to allow us to explore during the research process. We would also like to express our sincere gratitude to our Chalmers thesis supervisor, Mohammad Farsi, for his advice and input which were of immense value throughout the course of our project helping us stay on course. We would also like to thank Göteborgs Polis for their help in public relations in regards to our testing in central Göteborg. Additionally we would also like to thank Michael Ardenheim, the groundskeeper at Göteborgs Domkrykan for allowing us access to the cathedral to take tests at altitude. Last but not least, we would like to express our most profound gratitude to our families, whom without their love and understanding, this accomplishment simply would not have been possible.

Erik Higbie and Karam Akar, Gothenburg, February 2021.

Contents

List of figures

List of tables

1
Introduction

Internet of things (IoT) mesh networking is popular with its various applications in vehicular, home, industrial automation, and city monitoring/control applications. This project is to conduct a feasibility study for implementing a quasi-static LoRa mesh sensor network system in an exposed radio frequency (RF) setting in the area of Gothenburg city and analyzing the different connectivity parameters. The mesh implementation is the unique element that will allow all nodes to share information across the network rather than the traditional flow from a single node to the base station, extending both range and robustness. The LoRa protocol has several unique challenges: low data rates, high latency, ground-level node placement, and limited communication time that injects different challenges compared with other shorter range, higher throughput technologies in a mesh architecture. The aim of this study is to expand the research and development in the field of long-range IoT mesh sensor systems into the urban setting and highlight the viability and weakness of this type of deployment.

1.1 Background

IoT has some truly transformative potential in today's modern world. The ability to scatter sensors that use low power over a wide range has potential in several applications such as to track water levels in the event of flooding or register gunshots in neighborhoods or even something as mundane as tracking cargo containers at a port to speed up the delivery of a Christmas present [3]. Networks value is measured by the value of the data it handles but it is worthless if the data cannot reach its destination or is too expensive to transmit. This is where a network like the one presented in this thesis is useful. It is low cost and separates from other potentially more expensive options like cellular and LoRaWAN networks [4]. By investigating the ability to use LoRa in a mesh network like the one presented could open up the potential for whole new custom and or private deployments of sensors that are robust and highly flexible in modern urban environments where the use case can be any number of applications that require long-range, optional low power and don't need very high data rates.

1.2 Related work

One of the limitations of LoRaWAN presented in its single-hop nature was addressed [5], where their solution implemented building a proof-of-concept routing protocol to

enable mesh networking between LoRa gateways. Applications like Urban drainage system performance monitoring and real-time data gathering can be a handful of tasks due to the remote locations' nature and harsh RF environment. Thus, a synchronous Lora mesh network [3] was developed to enable more efficient communication with sensor nodes placed in such locations where LoRaWAN can face low penetration rates for nodes positioned in range-critical situations like sewers as well to increase the reliability of transmission and flexibility of deployment. In a similar deployment for underground and open-pit mines [6], high coverage and network Quality of Service (QoS) metrics are vital to providing real-time monitoring and push warnings in case of intrusions. We can see the benefits of mesh routing instead of the centralized topology of LoRaWAN in urban areas where connectivity was limited by signal attenuation even in campus-scale implementations where LoRa mesh-networking devices [4] showed a significant improvement in packet delivery rate.

1.3 Purpose

The purpose of the project was to create a demonstration and evaluate the feasibility of a long-range mesh sensor system using a custom network stack utilizing the LoRa communication protocol in an urban environment at ground-level while comparing the network functionality to a LoRaWAN network operating on a star topology. The network proposed by this report is to serve as a viability study and potential proof of concept along with a demonstration of one potential implementation of such a network with several unique criteria. These criteria are loosely based on a small fleet of e-scooters in the city while also providing the flexibility for other potential applications like various smart city services [7]. The criteria targeted by the goals that were, more concretely, fault tolerant network creation and recreation, 50 meters of node movement, a packet success rate of 90% of LoRaWAN, a network range of 1 km in the urban setting given the approximate 3 km range of LoRaWAN devices usually in urban environments, at least 50% packet throughput compared to LoRaWAN when the network is active, automated provision of a new device and network updating handled by the gateway and network capacity of a minimum of a dozen nodes per gateway.

1.4 Proposed approach

With the constant escalation of the number of connected devices operating within networks in urban settings, Infotiv and other users are looking to either have a backup network for sensors or deploying sensors in such a way where they are not completely dependent on external networks to collect data. The traditional solutions to this are either cellular connections that are power hungry and monetarily expensive or LoRaWAN, which necessitates the installation of a stationary base station serving as the single node of contact to all nodes in the network. The main goal was to determine if a different and potentially better solution to this problem exists through a distributed LoRa mesh network.

1.4.1 Environmental connectivity data gathering and analysis

The connectivity for Point-to-Point (P2P) communication will need to be evaluated on both a general and scenario level in order to determine the design and performance of an eventual LoRa network deployment. Therefore, this paper will produce testing data for Central Göteborg and show how the environment will impact said performance and design and thereby possibly lay the groundwork for more detailed modeling of ground-level LoRa communication for the future. Many studies have been conducted in urban spaces previously [8]. The key difference here is the ground-level communication between nodes which is what is required from this network given the mesh functionality. From these, a simple model based on the statistical characteristics of the connectivity data will be created to help provide broadened insight and serve to validate or invalidate the notion of generalized testing and positioning. This will also help determine the viability of placing such a network in such an environment.

1.4.2 Network creation, deployment and evaluation

This thesis presents the necessary building blocks to design and deploy LoRa mesh networks in urban environments separate from LoRaWAN implementations utilizing a single base station and the benefits and weaknesses of such a system. For this approach to be viable, the network needs to function in the environment of central Göteborg described in the data above, have some scalability against the increasing amounts of real data handling while displaying the properties of self-healing and adaptability despite constant change in the network. This viability will be evaluated by the design and then operation of a relatively simple custom-designed mesh protocol in a variety of tests. Additionally, the network will have certain requirements that depend only on its performance but also the restrictions of the LoRa Protocol and governmental regulations of the operating spectrum. The design of a mobile IoT sensor system with a mesh network needs to fulfill the following requirements.

1. Have robustness to interference and node failure and movement
2. Synchronization of packet exchange through routing protocols or whole network information sharing via flooding
3. Scalability of implementation of dozens of sensors
4. Accommodate node movement up to 50 m before network recreation is needed
5. Extend coverage in urban Göteborg for up to 2 km using relays
6. Extend the sensor's battery lifetime of up to several months
7. Be able to maintain network operation and fault tolerance without the need for an application server after network initialization
8. Device provisioning handled by using an application-level database
9. Flexibility with where a data sink can connect to the network
10. Abide by duty cycle restrictions for the spectrum in use
11. Utilize communications protocol specifications to allow for variable data rates dependent on conditions
12. Have interoperability with larger LoRaWAN gateways and applications[7],[9].

If the network cannot fulfill these restrictions then it will be concluded that this implementation is lacking and based on performance, further research and implementations will be suggested. This network should be deployed using the available hardware described in the equipment section and be further simulated using network simulation software to test device number limits.

1.5 Scope and limitations

This project had several varying criteria in the design of a network that are unreasonable to investigate within the time and resource limits placed on the project.

- The physical testing of the network will not expand beyond the hardware already described due to cost constraints. Other hardware implementations also won't be considered outside of Pycom modules.
- The power requirements of devices will be theoretically calculated but not experimentally measured. Additionally, this physical testing will not allow for the movement of more than two nodes at a time at a speed greater than stated above due to logistical challenges. Range testing greater than three hops will not be conducted. Connectivity measurements will not be highly granular nor cover all of Central Göteborg given time and accessibility limitations. Due to battery limitations, pushing data in the network outside of predetermined time frames will not be considered. A custom application is not planned to be addressed unless necessary.
- Channel compensation will not be researched or attempted given the robust nature of the LoRa protocol. The channel will not be measured using the USRP beyond the Infotiv office, located at Västra Hamngatan 8 Göteborg, given logistical and power delivery constraints.
- Sensor coverage will also be overlooked in this paper as this is not applicable to the demonstration.
- The network will not be simulated and only practically tested due to timing constraints for the project.
- Area Testing will be conducted in motion and Doppler frequency spread will not be taken into account given the frequency robust nature of the LoRa protocol
- Area and mesh testing at altitudes above the height of an average person i.e. (2 meters) will not be conducted due to timing and access limitations
- Area testing will cover a majority but not all possible locations within the proscribed area in light of time limitations
- Connectivity modeling will be limited to simple conclusions based on statistical analysis from gathered data and not designed in a user-orientated fashion or for practical application
- Advanced routing techniques will not be considered due to the limited nature of the LoRa protocol and time and knowledge limitations
- Various power levels and frequency bands will not be considered due to the increasing testing required being outside of the time allowed for the project and in potential conflict with legal restrictions

- Node positioning during testing will be as close to the desired points and placed on physical objects in the vicinity. Thereby positioning will not be consistent during testing between physical testing locations.
- Security concerns beyond DDOS and relay attacks will not be considered as other concerns are too far from the focus of the project. Security Implementations will be restricted to encryption and authentication on the physical and application layer protocols.

1.6 Tools and equipment

1.6.1 Communications hardware

The hardware used to run the communications protocol and the mesh networking is the 1st generation LoPy Board that runs Wifi, Bluetooth and, LoRa using an ESP32 microcontroller and a Semtechs SX1272 LoRa Modem [10]. These are programmed via MicroPython and have the ability to communicate P2P using the physical layer LoRa protocol with a custom network layer and additionally as nodes in a LoRaWAN network and as a nano-gateway to act as a LoRaWAN gateway. These boards are then connected to an omnidirectional 1/2 wavelength whip antenna designed for 868/915 MHz [11]. The LoPy boards are also connected to 4 AA batteries via a DC-to-DC down step converter to provide a steady 5 volts to the boards. The boards are programmed via Expansion Boards that connect via Serial USB connections to VS code.

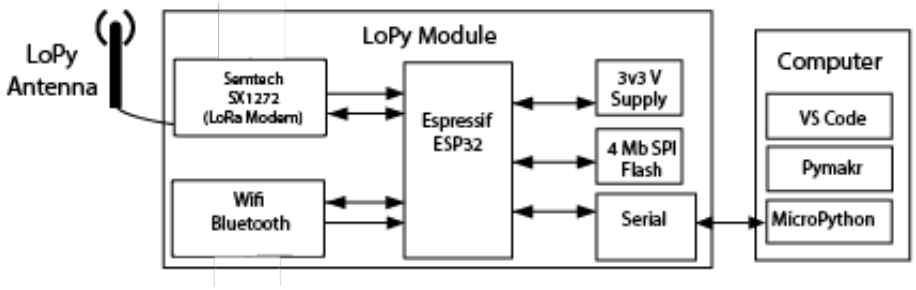

Figure 1.1: Block diagram for LoRa hardware

1.6.2 Evaluation hardware

To evaluate the RF characteristics of both the channel as well as the LoRa Transmitters an N210 USRP with a WX daughter board from Ettus is used as a mixer which allows for upconversion and sampling of the 868 MHz band [12]. The N210 block is where the analog to digital conversion as well as the different signal processing computations is handled utilizing the FPGA and allowed to the network through a Network Interface Card. The same antenna was also used for the LoPy boards. This USRP has been used with Matlab to gather and analyze information collected.

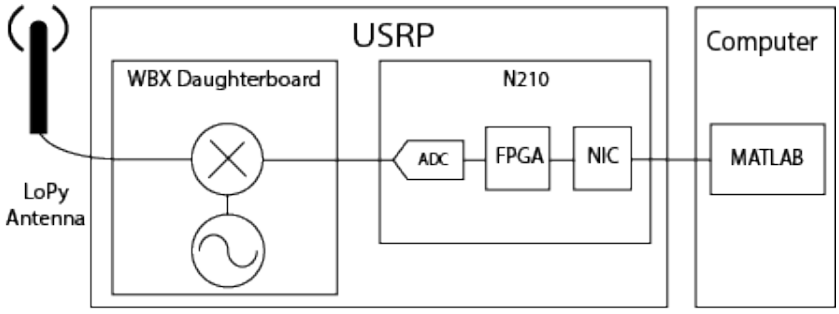

Figure 1.2: Block diagram for USRP

1.6.3 Software

Visual Studio Code is the primary IDE used for programming the LoPy boards, which are coded using MicroPython [13]. MicroPython is a Python wrapper for C99 code, which allows for the usage of most basic python libraries and code structure. [14] For the data analysis and connecting to the USRP, Matlab is used, which is a programming language with specialized tools for signal analysis and statistical analysis [15]. A network simulation software needed to be chosen to run network simulations, but was later removed from the scope of thesis.

1.7 Contribution

The contribution of this thesis would be in evaluating the ground-level performance in an urban space of the 863-870 MHz band typically used by long-range IoT devices. This would define the viable 'space' of these types of systems allowing future use cases to be designed around these criteria. Additionally, the creation and evaluation of a simple model for connectivity would shine light on the complexity of wireless connectivity at ground-level in urban environments.

1.8 Report outline

Chapter 2 covers the relevant theory in this thesis. The theory covers the basics behind the LoRa and LoRaWAN protocol, basic communication theory, mesh networking, and path loss aspects of wireless connectivity as well as the statistical metrics.

Chapter 3 covers the methodology used in this thesis. It also presents how the Pycom modules were set up to run LoRa and LoRaWAN, how the connectivity testing was conducted and the simple connectivity model was designed. Finally, how the mesh network was implemented and subsequently tested is also be detailed.

Chapter 4 covers the results of the tests presented in the methodology as well as how statistical measures of the data gathered in addition to describing the model criteria.

Chapter 5 discusses the results in more detail and elaborates on the veracity of the testing and network design as well as discusses their viability.

Chapter 6 elaborates on how future work could expand or apply the conclusions found by the report.

Chapter 7 contains conclusions drawn from the discussion in Chapter 5 thereby making a determination of the viability of the demonstrator.

2
Theory

2.1 Wireless sensor networks

A fundamental application of the LoRa standard has been deploying low-power devices that can communicate with each other or a base station at long ranges [16]. This type of application is typically called a Wireless Sensor Network which is important to introduce to frame other discussions and stated requirements properly, although this section only provides an introduction to the subject with a few nuances applicable to an urban LoRa network. A Wireless Sensor Network is a network of a large number of sensor nodes deployed to collect information from the environment or itself which is then sent through the network to a sink node for collection and analysis.
While the use case and sensing requirements dictate many of the challenges and trade-offs of a WSN, the connectivity requirements are also a critical aspect to take into account as without stable communication, the information being gathered cannot be recorded or analyzed. This connectivity requirement impacts primarily the scalability, energy efficiency, QoS, and range [17] [18].

2.2 Communication theory and performance

Communication theory is the science of the transfer and storage of information from one place to another. At its simplest, the process starts with bits which are simple 1's and 0's like an on-off switch. Sending bits from one place to another is never a guaranteed process as each time bits are transferred, they go through what is called a channel. Channels can be everything from a physical medium like paper to electronic conduits like wires to the air itself through which radio and sound waves propagate. Since this paper focuses on wireless communications, the channel of interest is the air with bits being carried on radio waves of certain frequencies. Information is encoded on these radio waves by altering them in terms of amplitude (power), phase (the shape of the wave at a certain point), or frequency (the number of times the wave oscillates per second). Radio waves that are pure sinusoids at specific frequencies have the unique property of being completely orthogonal allowing them to be layered over each other without corrupting each other. This means that bits encoded in a wave of a certain frequency or frequencies are able to be layered on higher frequencies called carrier frequencies. This then gives them the properties of the higher frequencies. As information, like bits on radio waves, travel through their channel, they always encounter a corrupting effect which typically impacts the

strength of the signal in the case of radio waves. This, combined with the noise of the environment captured at the receiver, can possibly lead to the erroneous decoding of the information. This effect is at its simplest described by the Shannon Hartley theorem show in 2.1 [19].

$$C = Wlog(1 + \frac{P}{N_0 W}). \tag{2.1}$$

As the above equation shows, noise affects the probability of whether the bit will change as it passes through the channel. Noise is often described as affecting a signal in a probabilistic fashion with varying estimated values, variance, and distributions. This makes the identification and understanding of the impact of noise on a communications system essential in order to understand how the system will behave. Bit error rate (BER) is described as how often noise affects a bit that it changes erroneously or in error. The BER defines how well a system can communicate as error necessitates re-transmission or lead to a system that cannot communicate at all. Bits are typically packaged in packets which is a group of bits grouped together to store information. These packets can be compressed which correlates extra information in the larger patterns of the bits in addition to having the bits be coded which also means that information is correlated in the larger patterns of the bits to allow for recovery in case of a bit error [20].

2.2.1 Networks and open systems interconnection layers

Often information that is being transmitted from one place to another lacks a single direct communications channel necessitating the need for a network of nodes that transport information from its origin to its destination. This network is often described in terms of the open systems interconnection (OSI) model which partitions the various aspects of the communications model into seven different layers. These are shown in figure 2.1 and start with the physical layer, which is where the hardware is typically grouped along with any software that handles the individual bits. Next is the data link layer which handles the grouping of bits into what are called frames along with most error correction checks and Medium Access Control (MAC) procedures that dictate the destination of information in a P2P format. Following that is the network layer which groups frames into packets and attaches them to information that allows them to be routed by other nodes in the network getting them from source to destination. Above that is the transport layer which acts as a handler between the upper levels and the network layer by breaking down larger data streams into segments, sending them through certain sockets attached to the network and makes sure that said segments can be properly recreated after transmission and handling any errors with the network layer if necessary. It is the first layer with a destination to source understanding as compared to the previous layers which handles strictly node to node communication. Lastly are the final three layers, the session layer, the presentation layer and the application layer which all serve to handle data creation, high-level data exchange or translation between standards if necessary, data storage and user presentation. The user typically only sees the application layer when communicating with modern networks [20].

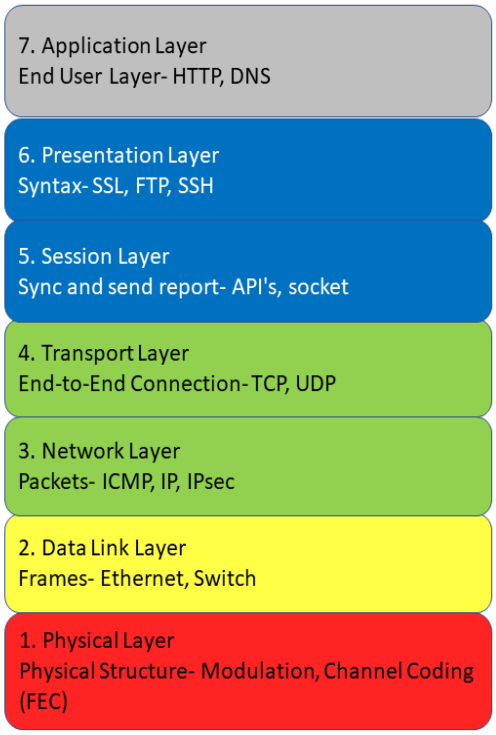

Figure 2.1: OSI model

2.3 LoRa

LoRa, stemming from Long-Range, is a proprietary wireless communication protocol residing on the physical layer of the OSI communication model. It was developed by Semtech based on earlier modulation schemes to meet the ever-changing and growing demand for low-power, stable-long range communication in M2M and IoT network devices. LoRa operates under the one GHz unlicensed ISM (Industrial, Scientific and Medical) radio band available for use worldwide [21].
LoRa is a product of the evolution of spread spectrum modulation technologies dating back to the 1950s where it was used for radar and military purposes due to its ability to avoid intentional and unintentional interference [22]. It uses chirp spread spectrum (CSS) which mainly comprises of spreading a certain information signal of narrow bandwidth into a wider spectrum while distributing the energy density uniformly throughout the band keeping the same energy consumption levels (even lower than most) but adding what can be kilometers to the range of transceiver coverage. This makes it also incredibly reliable and robust against co-channel noise, and insensitive to frequency offsets. Forward error correction with a redundancy factor between 1 and 4 to protect the data is implemented along with whitening (randomizing) of the generated sequence before modulating the signal [21]. Properties like long-range, low power, reliability and robustness to noise along with the low data rate requirements for operating sensor network nodes makes LoRa a great physical layer wireless communication protocol for building IoT application systems where uplink communication is key.

2.3.1 Chirp spread spectrum

Lora operates using a derivative of the modulation technique called chirp spread spectrum which allows for data that would have normally been sent using a certain frequency bandwidth to be spread out over a larger spectrum as can be seen in figure 2.2. This results in the data being sent with a similar power per hertz as the noise occurring across the channel. When information is sent in this way, the signal becomes highly robust to not only channel noise, but also multipath fading given the large frequency spread and Doppler shifting since a frequency shift of a few dozen Hz does not intractably corrupt the signal. This method also highly contributes to reducing the complexity of the receiver as the timing and frequency offsets will be approximately similar. The way this works is that the carrier signal constantly 'chirps,' rising or falling through the entire channel bandwidth and then jumping back to start. This can be seen through the frequency waterfall chart below. Information is encoded by interrupting this constant chirping process and restarting the chirp at a different frequency for the next chirp cycle.

2.3.2 LoRa PHY layer and modulation

LoRa is a low power, long range communication standard that operates in the unlicensed bands under 1 GHz (differs for different regions). In the Swedish Region where the demonstrator is being developed the band allotted is 863-869 MHz. Different restrictions imposed on the transmissions limits the duty cycle to 1% per node as well as putting a limit on the payload size.
LoRa uses chirp spread spectrum which mainly comprises of spreading a certain information signal of narrow bandwidth into a wider spectrum while distributing the energy density uniformly throughout the band keeping the same energy consumption levels (even lower than most) but adding what can be kilometers to the range of transceiver coverage. LoRa uses different channels for upload (125 kHz) and download (250 kHz) which makes it easier to abide by the duty cycle regulations of limited air-time per node of the network.

2.3.3 LoRa demodulation

A LoRA modem first modulates the data signal using a proprietary chirp spread spectrum method, which widens the bits in the frequency band depending on the spreading factor chosen which trades of throughput for energy consumption and range. The LoRa packet frame is divided into pilot and synchronization symbols, a header with the frame information and a variable payload that contains the data ended with a cyclical redundancy check (CRC) for error detection [23]. This modulation technique uses wide-band linear frequency sweeps over the allotted bandwidth (whether over 125 kHz, 250 kHz or 500 kHz) called chirps to encode information. The sweep can range from minimum to maximum frequency and are called up-chirps or reversibly from max. to min. which will then be a down-chirp.
When information is sent in this way, the signal becomes highly robust to both channel noise and multi-path fading, given the significant frequency spread and Doppler shifting. A frequency shift of a few dozen Hz does not corrupt the signal.

This method also highly contributes to reducing the receiver's complexity as the timing and frequency offsets will be approximately similar [22]. In the following figure, with frequency and time as our x-axis and y-axis respectively, the waterfall spectrogram of the LoRa signal picked up by the USRP where the pilot pattern of up-chirps, followed by two frame synchronization down-chirps. After the sync, data can be seen.

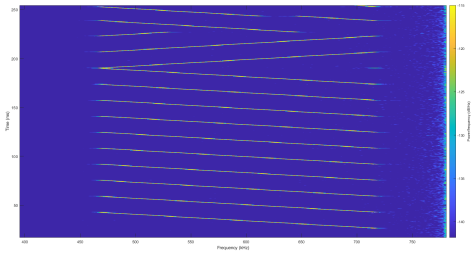

Figure 2.2: LoRa chirps captured by USRP

Information is encoded by interrupting this constant chirping process and restarting the chirp at a different frequency for the next chirp cycle. The input data is modulated on the higher rate chirp signal, R_c, which is the total selected bandwidth. The spreading factor (SF) controls the symbol's distribution over the signal, is an integer value in the range of 6 to 12 [22], [24].
Thus R_s, the symbol rate :

$$R_s = 2^{SF}/BW \tag{2.2}$$

Another advantage of the LoRa protocol is the low complexity of the required receiver. The message consists of a preamble pilot to alert the receiver of incoming data [22]. An important factor to consider is the synchronization, which is made to tune the receiver precisely for the chip alignment. The incoming signal is demodulated by multiplying with separate conjugate up-chirps and down-chirps. The result is a constant frequency component, and using Fast Fourier Transform, the component with the most power and the intended symbol will be determined

2.3.4 Use cases and implementations

LoRa technology characteristics of long-range, low power and high tolerance to noise bring it forward as a candidate in many wireless wide area network IoT applications of small and large-scale like Industry 4.0, smart city projects, logistics, tracking, etc. In these unusual circumstances due to COVID-19, LoRa can help facilitate safer operation in offices and workspaces by providing solutions to increase facility hygiene, ensure social distancing and monitor air quality. LoRa IoT deployments began in Helsingborg, Sweden, include a LoRaWAN network and is planned to extend throughout the country. Other LoRa use cases around the world include smart water-management solutions in Spain and India [25].

2.4 LoRaWAN

LoRaWAN is the open standard protocol added on top of LoRa layer. It facilitates addressing, networking and application functionalities like managing security, medium access, node provisioning and so forth. LoRaWAN specification, developed by Semtech and part of LoRa alliance, is designed for providing low power, wide area networking and support for two way secure communication across devices that are battery operated in order to serve IoT, Machine-2-Machine (M2M) and smart grid applications [26]. LoRaWAN employs a centralized architecture, which means all communication can occur only through a gateway (nodes can not talk to each other), which is also responsible for connecting the nodes to the network infrastructure through the internet or cellular backhaul like seen in figure 2.3.

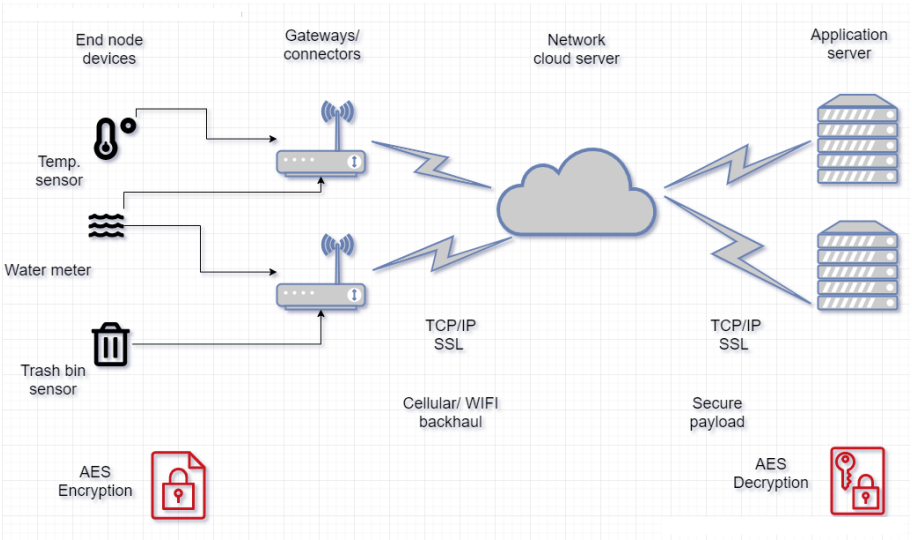

Figure 2.3: LoRaWAN architecture

2.5 Statistics

Given the inherently random nature of noise in communications networks, this means that communication links and networks will always have a degree of randomness associated with them [19]. This randomness is accounted for by using statistical models which allow for the characterization of such systems and the phenomena that affect them. These take the shape of random variables which are functions that show the likelihood of certain values occurring as the result of an experiment or event. This distribution is shown often as a probability density function (PDF). Arguably the most commonly occurring and used distribution is the Gaussian distribution shown in (2.3).

$$f_X(x) = \frac{1}{\sqrt{2\pi\sigma^2}} \exp(-\frac{(x-m)^2}{2\sigma^2}) \tag{2.3}$$

The Gaussian distribution is often used to estimate a range of random phenomena such as thermal noise, which is the root source of noise in basic communications

models. When considered as a function of an external variable such as time or space, these random variables become random processes [27].

2.5.1 Random variables

There is a range of random variables, several of which are listed below, that occur besides Gaussian distributions which are able to better model a variety of phenomena. The most basic of these are Uniform Random Variables, who's PDF is shown in equation 2.4, where all values across a range are equally likely to occur.

$$f_X(x) = \begin{cases} \frac{1}{b-a}, & a \leq x < b, \\ 0, & \text{elsewhere.} \end{cases} \tag{2.4}$$

An expansion on the Gaussian distribution as shown in 2.3 are Log-Normal Random Variables which are the exponential of a Gaussian distribution as shown in 2.6.

$$f_X(x, \mu, \sigma) = \frac{1}{x\sqrt{2\pi\sigma^2}} \exp(-\frac{(ln(x) - \mu)^2}{2\sigma^2}, \tag{2.5}$$

$$f_{X_{dB}}(x, \mu_{dB}, \sigma_{dB}) = \frac{1}{\sqrt{2\pi\sigma^2_{X_{dB}}}} \exp(-\frac{(x_{dB} - \mu_{X_{dB}})^2}{2\sigma^2_{X_{dB}}}. \tag{2.6}$$

This can be summarized simply as the Gaussian distribution of a variable defined in dB. The following two listed here, the Rayleigh and Rician distributions, are closely related to each other with the Rayleigh being a special case of the Rician where the a value in the Rician case being zero. Both, unlike Gaussian distributions are single-sided and typically used when studying wireless non-coherent communication systems as described in section 2.6.2.3. These two distributions are shown below with equation 2.7 showing the Rician distribution and equation 2.9 showing the Rayleigh distribution.

$$f_X(x, \sigma) = \frac{x}{\sigma^2} \exp(-\frac{x^2 + a^2}{2 * \sigma^2} I_0(\frac{as}{\sigma^2})u(x) \tag{2.7}$$

$$I_0(x) = \frac{1}{2\pi} \int_{2\pi}^{0} e^{x\cos(\Theta)} d\Theta \tag{2.8}$$

$$f_X(x, \sigma) = \frac{x}{\sigma^2} \exp(-\frac{x^2}{2 * \sigma^2} u(x) \tag{2.9}$$

Lastly, the power distribution $X^2_{Rayleigh}$ of the Rayleigh distribution takes the form of the exponential distribution which is shown below in (2.10) where λ is μ.

$$f_X(x; \lambda) = \begin{cases} \lambda * e^{-\lambda * x} & x \geq 0 \\ 0 & x < 0 \end{cases} \tag{2.10}$$

2.5.2 Monte Carlo simulation

The Monte Carlo Simulation is a method of 'brute force' to combine multiple distributions. Probability distributions that are combined either the same, different or

a combination of probability distributions rarely has defined probability distributions as a result. Gaussian distributions are a common exception given their linear nature allowing them to be added together to form further Gaussian distributions. However, for other distributions, combining either requires complex math such as convolution for the addition of independent distributions. To avoid this, a tactic is to generate a large number of samples from the first known distribution and then use those values as 'seeds' (or means) for the following distributions to generate a large number of samples per 'seed'. The result is a large number of values that roughly mimic what would have been a probability distribution if a mathematical combination was possible. While computationally difficult, Monte Carlo simulations allow for the analysis of models that otherwise would be difficult or impossible to generate purely mathematically [15].

2.6 Urban path loss

Wireless connectivity in an urban setting has significant differences from a lab setting or even a rural or suburban setting. In Sweden, the location of the testing site, urban is defined as an area of 200 or more inhabitants where the buildings are no more than 200 meters distance from each other [28]. Such an environment creates significant issues with the propagation of wireless signals particularly in regard to path loss and interference [29]. Among these issues are shadowing by objects such as buildings and vehicles, multipath fading as a result of signal reflections off of obstacles and noise/interference from other competing broadcasts. This is in addition to other more universal effects such as ground reflection loss, Doppler shift, and standard signal Free Space Path Loss (FSPL).

2.6.1 Free space and simplified path loss

FSPL is the result of the signal dropping in power density over distance as the signal spreads out over a greater area. This decrease in received power is fairly well established by the FSPL model shown below in (2.11) where P_t is the power transmitted, Pr is the power received, G_l is the gain of the receiver and transmitter's antenna and amplification, λ is the signal wavelength, and d is the distance between the transmitter and receiver.

$$10 * log_{10}(\frac{P_t}{P_r}) = -10 * log_{10}\frac{G_l\lambda^2}{(4\pi d)^2} \tag{2.11}$$

FSPL works well in environments where there are no obstructions between or near the transmitter and receiver which have Line of Sight (LoS) in a straight line between each other. However, when this is not the case, several other phenomena have an impact on path loss [30]. In the case of non-ideal situations and real-world scenarios, a model called the simplified path loss model can be used. It takes into account a rough assumption of the space and estimates what would be considered to be the signal power loss. This is however a broad average and typically a very rough estimate of the connectivity conditions. This model is shown in equation 2.12 where

d_0 is the reference distance and γ is the path loss exponent that effectively averages out the impact of the environment in terms of scattering and shadowing.

$$10 * log_{10}(\frac{P_t}{P_r}) = -10 * log_{10}\frac{G_l\lambda^2}{(4\pi d)^2 * (d/d_0)^\gamma} \tag{2.12}$$

2.6.2 Stochastic signal fading

When radio waves come into contact with objects, they are reflected and absorbed to varying degrees according to the type of the material, the wavelength of the wave and the angle of impact. All these factors make the understanding of how radio waves interact with complex environments very difficult. The most accurate way to approximate these factors in the far field, where $2d >> \lambda$, would be to ray trace the path of the radio waves as they travel from the transmitter to the receiver. However, this is incredibly difficult and computationally taxing, so a variety of documented phenomena have been approximated [30].

2.6.2.1 Ground reflection

The first of these is the ground reflection phenomenon which results from the radio waves hitting the ground and reflecting up towards the receiver's antenna. Figure 2.4 illustrates this issue which results in increased interference in the signal making the resulting path loss more erratic and generally higher as shown in figure 2.5, where h_t was 3.7m and h_r = 1.7m [1].

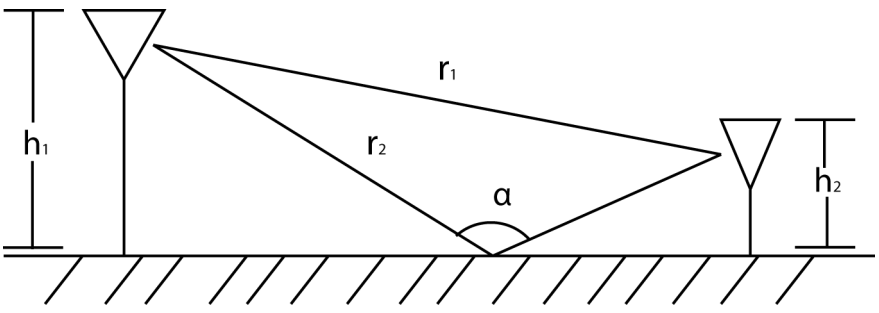

Figure 2.4: Two ray geometry for both direct signal path and ground reflection

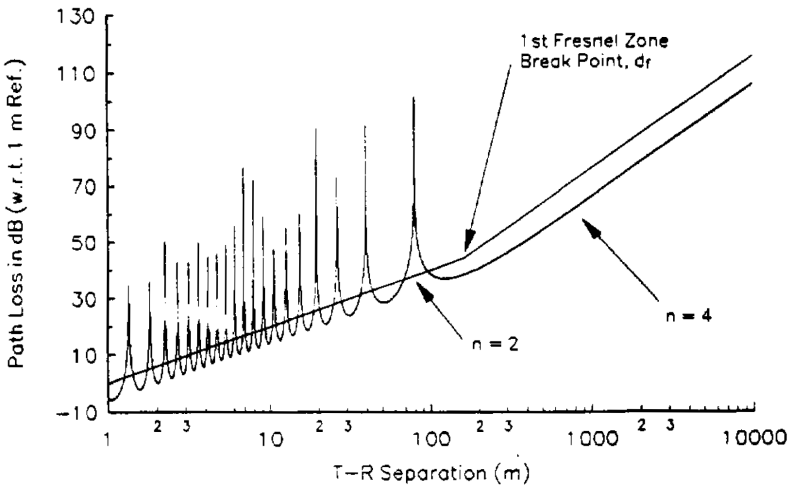

Figure 2.5: Path loss over distance for ground reflection fading [1]

However, the path loss does end up stabilizing at what is called the break-point distance. This distance can be calculated using (2.13) below in which d_f is the break-point distance and λ is wavelength

$$\begin{aligned} d_f &= \frac{1}{\lambda}\sqrt{(\Sigma^2 - \Delta\ 2)^2 - 2(\Sigma^2 + \Delta\ 2)^2(\frac{1}{\lambda})^2 + (\frac{1}{\lambda})^4} \\ \Sigma &= h_1 + h_2 \\ \Delta &= h_1 + h_2 \end{aligned} \tag{2.13}$$

The ways to avoid this issue is by raising the height of the receiver antenna or lowering the transmitter antenna making the resulting reflections off the ground at too low of an angle to be picked up by the receiver.

2.6.2.2 Fresnel zone; NLOS vs LOS

While ground reflection path loss is relatively stable at the distances considered, the concept brings up an important aspect to additionally consider which is Fresnel zone blockage.
The Fresnel zone is a zone that is typically modeled as an ellipse with the antennas as each foci. If objects are present within this zone, signals that are sent from an antenna that would typically not be a LoS component of the signal interact and diffract off of the objects within the zone, causing a phase shifting and similarly to multipath fading described below in section 2.6.2.3 results in signal inference and a loss of received signal power. The first Fresnel zone is described by equation 2.14, where r is the radius of the first Fresnel zone, d_1 and d_2 are the distance from the transmitter and receiver, respectively, and λ is the wavelength of the sent signal [31].

$$r = \sqrt{\frac{\lambda * d_1 * d_2}{d_1 + d_2}} \tag{2.14}$$

The addition of the various diffracted waves is very complicated and modeling this behaviour is outside of the scope of this report but it is important to note that as

long as more than half of the Fresnel zone is filled then it is reasonable to assume LoS parameters [31] [30].

2.6.2.3 Multipath fading

The second is multipath fading where the radio signals sent out from the transmitter reflect off of the surrounding environment which then reaches the receiver. Since these signals reflect off of various different surfaces at different distances and angles, they both interact constructively and destructively in addition to arriving at the receiver at differing times. The receiver then receives all of these reflections which range in phase with some reflections sharing similar phases and appear as another copy of the signal. This signal is therefore the sum of both the LoS signal and all multipath components as defined by (2.15), where $u(t)$ is the equivalent low pass signal and f_c is its corresponding carrier frequency. Additionally, $N(t)$ is the number of resolvable multipath components, each component paths length $r_n(t)$, their corresponding delay $\tau_n(t)$, their amplitude α, and their Doppler phase shift ϕ_{D_n} for each multipath component.

$$\begin{aligned} r(t) &= Re\left\{\sum_{n=0}^{N(t)} \alpha_n(t)u(t-\tau_n(t))e^{j(2\pi f_c(t-\tau_n(t))+\phi_{D_n})}\right\} \\ \tau_n(t) &= r_n(t)/c \end{aligned} \tag{2.15}$$

This combination of signals results in the receiver receiving echos of the original signal which then interfere with receiving any subsequent signals. This can be simplified by assuming that the delays of the multipath components, known as delay spread, are comparatively small compared to the length of the signal (inverse of bandwidth). This allows for the use of a narrow band fading model described by (2.16).

$$r(t) = Re\left\{u(t)e^{2\pi f_c t}\sum_{n=0}^{N(t)} \alpha_n(t)e^{-j\phi(t)})\right\} \tag{2.16}$$

By modeling it in this way, the lowpass signal $u(t)$ becomes independent of the multipath components and does not need to be considered to characterize the random path loss caused by multipath. This allows for the splitting of the signal into the in-phase and quadrature components which is shown in equation 2.17, where r_I is the in-phase component and r_Q is the quadrature component.

$$r(t) = Re\left\{\left[\sum_{n=0}^{N(t)} \alpha_n(t)e^{-j\phi(t)})\right]e^{2\pi f_c t}\right\} = r_I(t)cos(2\pi f_c t) - r_Q(t)sin(2\pi f_c t) \tag{2.17}$$

$$r_I = \sum_{n=0}^{N(t)} \alpha_n(t)cos(\phi_n(t)) \tag{2.18}$$

$$r_Q = \sum_{n=0}^{N(t)} \alpha_n(t)sin(\phi_n(t)) \tag{2.19}$$

$$\phi_n(t) = 2\pi f_c \tau n(t) - \phi_{D_n} - \phi_0 \tag{2.20}$$

If N is large and α and $\phi_n(t)$ can be considered independent random variables between different components, then r_I and r_Q can be considered to be jointly Gaussian

random processes which are both zero mean and equal variance since they have no deterministic scaling factor and similar distributions given their shared origin. With this assumption it is then possible to calculate the signal envelope of the signal $r(t)$ since adding the square of two Gaussian distributions and then taking the square root creates a Rayleigh distribution as shown in equation 2.9 [27]

$$Z = \sqrt{X^2 + Y^2} \tag{2.21}$$

$$z(t) = |r(t)| = \sqrt{r_I^2(t) + r_Q^2(t)} \tag{2.22}$$

Thus, the probability distribution function (PDF) of r(t) is equation 2.23.

$$p_Z(z) = \frac{2z}{\sigma^2} exp\left[-\frac{z^2}{2\sigma^2}\right] \tag{2.23}$$

This is where $2\sigma^2$ is the average received power of the signal's multipath components minus the FSPL and shadowing loss. That is also the λ value in Z^2 (the power distribution of (2.9), which is an exponentially distributed probability function shown in (2.10). This power distribution is achieved by substituting $z(t)^2$ with $|r(t)|^2$, which results in the exponential distribution shown below where $\bar{P}_r$ is the averaged received power.

$$P_{Z^2}(x) = \frac{1}{\bar{P}_r} e^{-x/\bar{P}_r} \tag{2.24}$$

Since these reflections are incredibly complicated they are typically described in probabilities in either a Rayleigh distribution for non LoS communication or in a Rician distribution for a LoS scenario. The Rician pdf is shown in equation 2.25 where s is is the power in the LoS component.

$$p_Z(z) = \frac{z}{\sigma^2} exp\left[\frac{-(z^2 + s^2)}{2\sigma^2}\right] I_0(\frac{zs}{\sigma^2}) \tag{2.25}$$

who's received power is $s^2 + 2\sigma^2$. As the environment becomes increasingly complicated, the K should decrease until it reaches 0 denoting the loss of LoS. Unfortunately, the power distribution of Z is not well defined unlike for Rayleigh fading.

The receiver should be ideally picking up the LoS signal if it exists and, if not, then the primary reflection. However, there are risks that the receiver may pick up echos from later in time resulting in small scale fading which reduces the power and corrupts the information carried by the signal. Research does show however that given a robust coding rate, LoRa shows significant robustness to multipath fading with only SF 7 showing any susceptibility as shown in the figure below 2.6 from an experiment conducted in an anechoic chamber with a metallic stirrer and a metal plate blocking LoS communication [2].

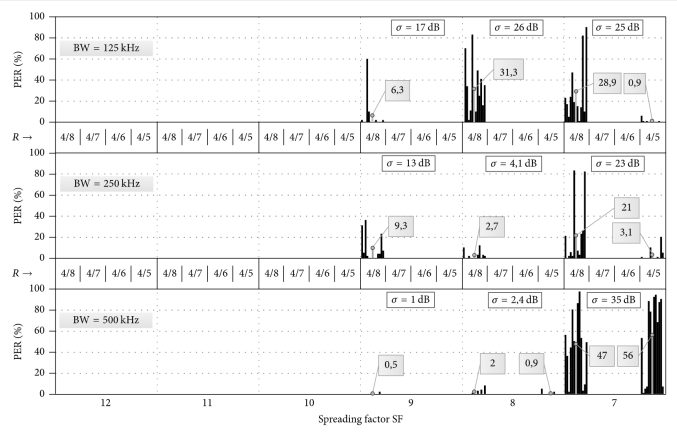

Figure 2.6: Multipath testing data [2]

2.6.2.4 Shadowing

The third of these is shadowing which is the result of obstacles in the path of the signal. This is a particularly detrimental form of fading as radio signals have difficulties in penetrating buildings in an urban environment and instead have to either take a significant power loss going through buildings or have to be reflected around by other buildings. While this type of path loss is often estimated with a γ value in the simple path loss model, this can be expanded with a stochastic model where the fading has a log-normal PDF which can also be written as a Gaussian distribution of decibels as shown in equation 2.26. P_t and P_r stand for power transmitted and power received respectively, $\sigma_{\psi_{dB}}$ is the standard deviation and $\mu_{\psi_{dB}}$ is the mean.

$$p(\frac{P_t}{P_r} = \psi_{dB}) = \frac{1}{\sqrt{2\pi}\sigma_{\psi_{dB}}} \exp\left[-\frac{(\psi_{dB} - \mu_{\psi_{dB}})^2}{2 * \sigma^2_{\psi_{dB}}}\right] \tag{2.26}$$

This model has a good amount of empirical support although the mean and standard deviation needs to be supported with empirical data often times for the most accurate prediction. It is also important to note that this model gives the average path loss irrespective of local deviations. This means a potential decorrelation where the model stops closely correlating and is typically on the order of the size of the buildings, groups of buildings or other obstacles. This is why the statistical model of shadowing should be based on a variety of different empirical samples at different spatial points in order to create as accurate a model as possible.

2.6.3 Doppler frequency shift

The Doppler shift is a shift in frequency of a radio signal caused by the transmitter or receiver moving in relation to the other which results in either a shift up of the frequency if the two are approaching each other and a shift down if they are traveling away from each other. This relationship is described by the Doppler equation in (2.27) where f is the observed frequency, f_0 is the emitted frequency, c is the speed of light, v_r is the velocity of the receiver, and v_s is the speed of the transmitter.

$$f = (\frac{c \pm v_r}{c \pm v_s}) f_0 \tag{2.27}$$

These shifts are comparatively small when compared to higher frequencies with the Doppler shift being around 100 Hz for frequencies of 1 GHz at speeds around 75 km/h

2.7 Wireless mesh networks

A mesh network is the result of the continuous evolution in the application requirements of mobile ad-hoc networks (MANETs) to fit the growing and changing need for data and connection.
A MANET is a network topology used to provide ubiquitous connection and bandwidth for a number of users/nodes, whether stationary or mobile, without the need to install a rigid infrastructure or have a pre-existing network configuration by allowing single, or multiple, wireless link hops between those nodes. The first MANET's date back to more than 30 years ago and were first developed by DARPA (Defence Advanced Research Projects Agency) [32] which was targeted to provide military applications as a part of the packet radio network (PRNeT) project in 1972. The packet radios supported spread spectrum, half-duplex communication. Routing protocols that ensured reliability, speed and correctness were implemented. And as radio communication research developed with improvements to WiFi technology (802.11) in the 1990's, commercial applications for MANET's on laptops became more and more prevalent eventually giving rise to wireless mesh networks (WMN).
In a similar manner to MANETs, WMNs provide a decentralized, peer-to-peer wireless connection service between nodes with multi-hop ability, but they require a more rigid infrastructure for network support because of their hierarchical approach to the network architecture as opposed to the flat structure of MANETs. The mesh routers tend to be generally static to provide connectivity to the nodes over a certain area. So one could say that a wireless mesh network is a specific type of mobile ad-hoc networks [33].
Mesh network's ability to self-build and heal through dedicated routing protocols makes them fault-tolerant, robust and highly adaptable. WMNs' hierarchical structure enables integration and interoperability with other networks by supporting multiple network access and wireless communication technologies, therefore, allowing for a high range of use cases. Depending on the application requirements, whether it is high bandwidth, reliability of communication or low-cost connectivity, the characteristic flexibility of WMNs make them an integral part of the IoT revolution where they are applicable in numerous services like disaster recovery, logistics of transportation and tracking, cellular backhaul, and smart city projects[34].

2.7.1 Architectures

WMN comprises wireless nodes or clients that are interconnected with gateways or access points. Each node acts as a router in transferring the data from one neighboring node to another until the packet reaches the network's access point.

This results in the hierarchical decentralized mesh network structure. Mesh networks can have 3 different types based on the purpose they intend to serve.

2.7.1.1 Infrastructure/Backbone mesh architecture

In backbone mesh, the network relies heavily on the interconnection of routers to act as access-points for the nodes as they have the responsibility of routing data and serving clients. They also integrate the mesh with pre-existing wireless networks and internet by performing bridge/gateway functionalities. This type of mesh networks serves infrastructure connectivity applications. The following figure illustrates a basic mesh infrastructure deployment and how it can serve multiple sub-networks.

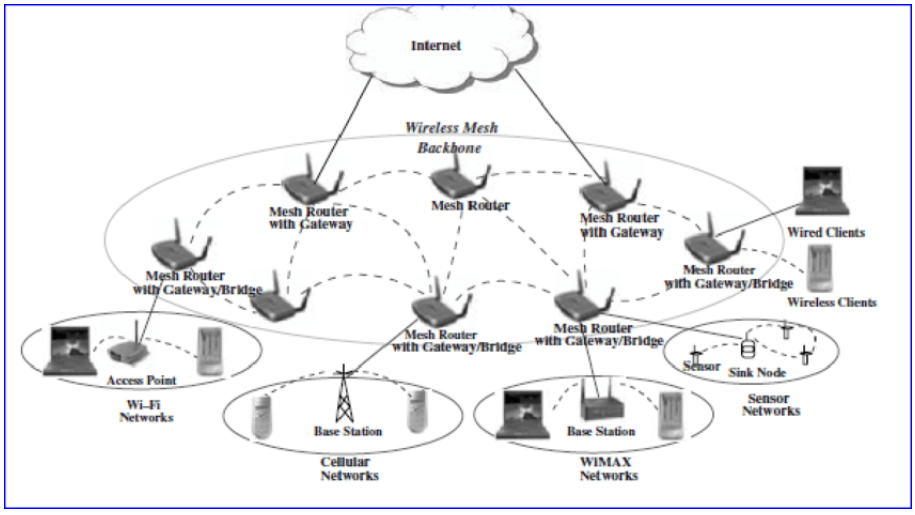

Figure 2.7: Infrastructure WMN
[35]

2.7.1.2 Mesh architecture based on clients

Mesh architecture based on the client have their client nodes serve the routing functionalities through P2P connections and provide the user-end applications are known as Client wireless mesh networks. There is no need for mesh routers in this type of networks as it is seen in the following figure.

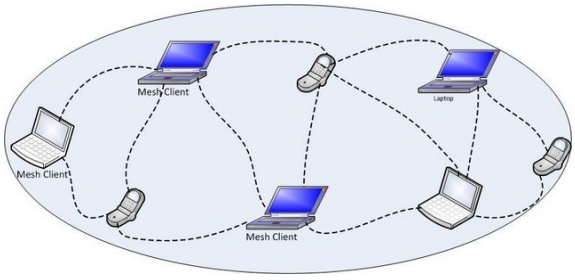

Figure 2.8: Client WMN
[35]

2.7.1.3 Hybrid mesh architecture

The combination of the prior two networks is known as a hybrid wireless mesh network, where the infrastructure connectivity links like WiFi or cellular is provided to the client nodes through mesh routers and gateways while also allowing the client nodes to access the network through P2P connection with other client nodes. Private mesh networks to serve sensor and monitory purposes usually deploy their own infrastructure and sub-networks to serve these applications as in the following figure.

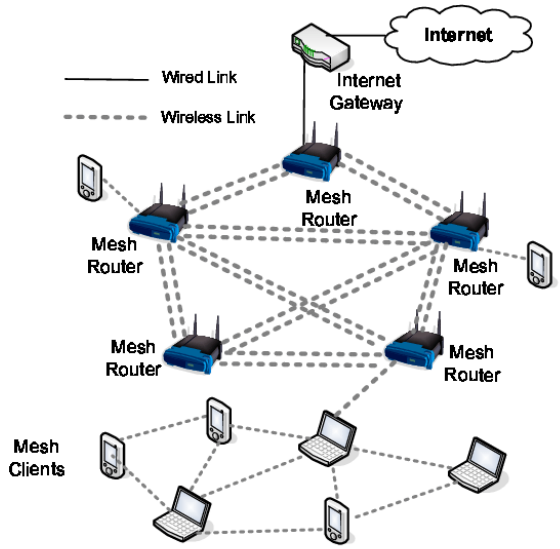

Figure 2.9: Hybrid WMN
[35]

2.7.2 Routing algorithm

Due to energy and air-time restrictions of mesh networks and the necessity for nodes to repeatedly discover and configure routes and pathways for packet forwarding because of their dynamic topology, this puts a great deal of importance on choosing the suitable routing protocol for the node operation. Picking the wrong protocol depending on the network's intended application may deteriorate the efficiency of transmission heavily and deem the network unusable. Routing protocols use software algorithms to determine optimal network data transfer and communication pathways between network nodes. Routing protocols can vary in complexity and functionalities depending on the requirements and can be generally categorized into 3 groups [36].

2.7.2.1 Proactive routing protocols

In networks that utilize a proactive routing algorithm, each node maintains one or multiple routing tables representing the complete topology of the network. These tables are updated regularly in order to maintain up-to-date routing information from each node to every other node. In order to keep an updated table, network topology information is exchanged regularly between the nodes, leading to high

control overhead traffic. On the flip side, routes will be available on demand which means no delay in communication. An example of a proactive routing approach can be Destination Sequenced Distance Vector Routing (DSDV).

2.7.2.2 Reactive routing protocols

Reactive routing protocols use route determination procedures. The on-demand routing protocols symbolize the nature of ad hoc networks, where high node mobility is needed. When a packet is to be sent between nodes, firstly, the path to the destination is discovered on the spot and then a connection is established. The procedure for route determination is usually done by flooding the network with route request packets. Even though flooding is a reliable method of spreading information over the network, it is bandwidth consuming with the increase in number of network nodes. Reactive routing approach uses broadcasts whenever a packet needs routing causing high latency but induces very little control traffic overhead and memory usage when compared to the proactive routing protocol. An Example is Ad hoc On Demand Vector Routing (AODV).

2.7.2.3 Hybrid routing protocols

Combining proactive and reactive protocol to fit the latency and control overhead limits of the network, i.e., small scale networks can maintain routing tables to utilize low delays while networks that tend to be larger in size can use on demand routing to decrease the load on memory and control overhead. This type of algorithm is best suited for the Zone Routing Protocol (ZPR).

2.7.3 Multiple access schemes

In half-duplex communication, meaning either transmitting or receiving at a certain time, one of the challenges of wireless networking using embedded devices is their limited radio capabilities. When the gateway and the nodes all must share the same medium, i.e., broadcast on the same Radio Frequency (RF) band, this poses interference and collision issues during detection. Thus, different techniques can be used to allow transmission with a minimum amount of packet loss while sharing the same channel. The first implementation is to dedicate separate time intervals for the devices to use the radio medium, meaning prevent them from transmitting simultaneously. This technique is called Time Division Multiple Access (TDMA). The challenge in this scheme is how to be able to time synchronize the different network radio devices in order to prevent overlap but also minimize the dead airtime as much as possible. Dividing the available frequency band into different channels to use by the transmitters can be a solution to packet collisions. This technique is Frequency Division Multiple Access (FDMA). FDMA was used in the first-generation(1G) terrestrial cellular systems, but it comes with an inherent disadvantage of the limited available spectrum to use and with the scaling of devices, it needs highly accurate filters in order to use closely adjacent channels without interference issues occurring. Another multiple access technique is Code Division Multiple Access (CDMA). It allows radio devices to transmit on the same bands simultaneously without in-

terfering with each other by using different code schemes. These codes are used to spread the signal over a wider bandwidth; thus, CDMA is considered as a spread-spectrum multiple access which can be highly robust to interference as long as the coding schemes used are orthogonal (codes correlation should be close to zero). This increases channel capacity which is controlled by the ratio of how much the data bits of the signal are spread over a wider frequency band which is called processing gain [37]. Wideband CDMA was used in 3G cellular technology. Other techniques that enable sharing of wireless communication medium exist like Spatial Division Multiple Access (SDMA) which can utilize numerous antennas and directed signal power.

3

Methods

This chapter details the testing methodology creation and the construction of the demonstrator. This begins with simple LoRa and LoRaWAN communication description in section 3.1 and then goes in to the details of the setup and implementation of connectivity testing for the communication protocol in sections 3.2 and 3.3. To gain insight into the data, various types of analysis was done on the results from the testing which is detailed in section 3.4 leading to the creation of the simple predictive connectivity model and the testing of the model which is explained in section 3.5.1. To wrap up the methodology, a deeper dive is done on the design of the network based on said data and testing of the network as described in section 3.6. Given the phased nature of the report, this chapter will, by necessity, refer to various sections in chapters 4 and 5 to give context to the methodology presented in later sections of this chapter.

3.1 Implementation of LoRa and LoRaWAN communication

The project's initial part was demonstrating a simple P2P communication using the LoRa protocol at the physical layer. This is relatively simple as most of the protocol is API driven and technical aspects like the pilot, SF etc., are handled by the microprocessor and LoRa modem. The goal should be packet transmission, successful reception and, subsequent acknowledgment. The next step to networked communication would be multi point communication between nodes with acknowledgment. However, this necessitates the implementation of some channel multiple access schemes to overcome the very likely possibility of crosstalk. The option that appears most viable is a combination of TDMA and FDMA as the LoPys are only capable of listening to one frequency band at a time but can receive and transmit on a variety of bands. Once implemented, it is easy to gather basic channel information such as packet success rate and SNR and RSSI through API commands. Once this basic communication was achieved, the LoRaWAN network protocol was implemented to act as both a test case and baseline for the custom protocol. While the protocol is self-contained and easy to deploy package, certain elements bear explanation below.

3.1.1 Regulatory limits

Given the inherently limited nature of the frequency spectrum in nature, the European Commission through the European Conference on Postal and Telecommunications' Electronic Communications Committee has harmonized a set of standards that divided this spectrum among a variety of uses [38]. For the purposes of this report, these standards are very important in that they dictate the way the LoPy modules can communicate in terms of frequency, bandwidth, time on-air, and transmission power. The specific standard that is applicable to the modules is Recommendation 70-03 dealing with short-range devices (SRD) and specifically, the first annex which regulates non-specific use case short-range devices [38]. LoRa uses the frequencies defined in the document between 863-870 MHz with LoRaWAN using the frequencies around 868 MHz. For this report, the frequency band of 869.4-869.65 MHz was chosen given its advantageous criteria of having a transmit power of 500mW effective radiation produced at the antenna and a 10% duty cycle for transmission time allowing the device to be transmitting for 6 minutes for each hour. Despite this being superior transmit power and duty cycle time compared to LoRaWAN, it was decided that this would provide a best-case scenario for this type of demonstration, providing a more robust conclusion on viability. These restrictions do present significant barriers to having a traditional always-on mesh network and making continuous live updates from sensors in a network significantly more difficult and practically nonviable.

3.1.2 Micropython and LoPy

As explained in section 1.6, the communications hardware used is built and programmed by the company Pycom. Their implementation contains a sizable amount of API functionality that proved invaluable in the creation of this report. As opposed to other common embedded electronics, the LoPy modules used ran a C99 wrapper using a simplified version of Python called Micropython that could interact with bare-metal functions of the chipset. While this functionality was not used in significant ways, the high-level nature of the python language did cause significant issues with memory handling, such as socket buffer with was used to gather data from the LoRa modem and hardware pins.

3.1.3 LoRa PHY layer communication using MAC addressing

Communicating between LoPy modules is done at the lowest level by using the LoRa physical layer protocol with MAC addressing. The step-by-step process to do this is detailed in the Pycom documentation but the basic steps will be laid out here [39]. The modules uses API commands that are processed by espressif processor which translates these commands into bit signals to the LoRa modem which handles all transmission and reception of the wireless LoRa signals. The modem is initialized by creating a LoRa object with a variety of various properties of which the operating mode (LoRa physical or LoRaWAN), the operating region(EU, NA, Asia, or AUS), the frequency, the SF (7-11), the bandwidth(125 kHz or 250 kHz), forward error

correction coding rate (4/5,4/6,4/7,4/7), and the transmit power (2-20) are the relevant properties to LoRa communication at the physical and data layers. This object also holds information pertaining to the properties applicable to the last received and transmitted packets such as received packet timestamps, received signal strength (RSSI) in dBm, signal to noise ratio, transmit power, transmit time on-air, and packet counter among others. These properties are very important in data gathering in tests detailed later in sections 3.3, 3.5.1, and 3.6. The information that is transmitted is packaged in bytes and sent to a custom implementation of the python object socket, which sends the information to the LoRa modem which then codes the message and appends the necessary preamble and generates the RF signal for transmission.

3.2 Evaluation of LoRa packets structure and channel using SDR

An important part of evaluating the urban factor of the demonstration is to measure both the channel in terms of noise level and interference and to measure the effect of multi-path fading and other corrupting factors affecting the signal. This was done by using the URSP described in the section 1.6 connected to the same antenna used by the LoPy modules and connected to a computer running Matlab which served as the data sink and user interface for the USRP. The channel was evaluated by taking multiple long-term sample sets from the USRP and measuring the noise floor over the frequency being investigated in the later tests (868 and 868.4 MHz), any coloring of the mentioned noise floor and, any interfering signals and what strength they may have. The USRP is also used to take measurements of LoRa packets sent at various SFs to provide spectrograms of the sent packets to ease the explanation of the packet structure of the sent signal. Measurements of these signals were also attempted at longer ranges but the level of signal loss and insufficient processing power of the computers used made spectrograms and other measurements of this signals unpractical. The measurements of the urban channel were taken at the Infotiv offices with the antenna outside the window to ensure both an unimpeded measurement of the channel and a power source for the USRP. Noise measurements were taken over the course of an hour or more to gain a more time independent result.

3.3 Urban wireless connectivity data gathering

Any wireless network must maintain a reasonable connectivity stability in order to ensure the smooth flow of information. Without this, the usefulness of the network becomes incredibly limited. Thus, when performing data gathering tests, it was assumed to have a directionally agnostic channel, meaning the signal sees the same channel whether traveling from or back to a node [40]. To evaluate the viability of a demonstrator of a LoRa mesh network in an urban setting, the connectivity limits need to be explored and defined. This will be conducted via a series of tests

gathering connectivity data and then analyzing this data to draw conclusions from as described in 3.4. These tests are divided up into two groups, tests to calculate a rough effective range and tests that roughly evaluate connectivity over larger urban areas from multiple testing locations. While these testing protocols are not based on the established methodology for this kind of tests, as there are none readily available, there are grounded assumptions that support the methodology presented that will be explained as needed.

3.3.1 Physical setup

The LoPy nodes were powered using a 4 AAA battery pack and mounted on Infotiv scooters' stand which had a height of ≈ 1.2 meters like in the following figure. The scooters were used mainly to have as a close of demonstration to real life application as possible. Another reason was to speed up the data collection process allowing for more samples recorded.

Figure 3.1: LoPy rig

3.3.2 Effective range testing

In order to gain a basic understanding of the connectivity, the first round of tests was conducted with the main goal of establishing a distance at which there was an 80% packet success rate which would provide for a 50% packet success rate over 3 hops in a network. This measure was deemed acceptable for a worst case semi stable network communication. The location was chosen to act as a roughly average point in an urban setting with a reasonable LoS but with buildings surrounding and both roads, alleys, and a somewhat open space.

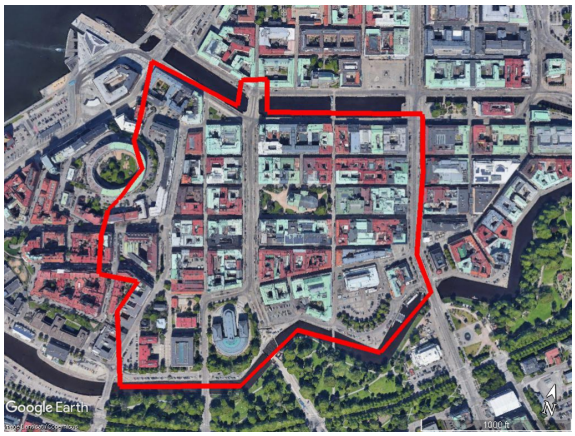

Figure 3.2: Effective range testing area

As can be seen in figure 3.2, the testing area of $\approx$ 460 square meters, within the red polygon borders, contains a blend of environments with open and closed spaces which should prove a good rough estimate for the effective range of LoRa urban ground-level communication.

Additionally, this proved a logistically advantageous measuring location given the nearness to the office here the analytic work was being conducted allowing for significant debugging of the testing hardware and software. These proved very difficult to get robustly working given the imprecise nature and lack of experience with LoPy and Micropython. The tests consisted of two LoPy modules, one acting as a stationary 'base station' (the base station) and the other connected to a mobile LoPy module (the node) that was attached to a backpack containing a laptop which when worn would move on an electric scooter to ease in mobility when testing. The base station was roughly 1 meter off the ground as shown in an example placement in figure 3.3.

Figure 3.3: Base station position example on the bike rack

The node then sent out a ping signal consisting of a packet with a dummy payload that would be received by the base station which would then send back a packet containing information regarding the statistics of the packet that was pinged out by the base station. This return signal would then be received by the base station and the same statistics would be derived from the return signal. The statistics would then be outputted via a serial connection to a connected computer and recorded in a CSV file for further analysis later. These tests were conducted at three SFs, 7,9, and 11 at two different times to reduce the temporal impact on the testing. The path taken to collect the data was chosen as it balanced the variety of environments and with sufficient distance while making the path as efficient as possible to reduce the time necessary for each test which resulted in data being taken primarily on roads or larger pedestrian paths. This results in a total of 6 tests, excluding testing necessary for debugging the software.
Traditionally these tests would be done with packets being sent in one direction rather than a round trip. However, as these tests are informing not only a path loss model but a general evaluation of the viability of network connectivity with both data and acknowledgments being integral to a network and the lack of hardware and time available for the testing, the ping and return method of measuring was decided as the most efficient in gathering larger amounts of data despite the potential issue of outage rates suppressing otherwise successful transmission.

3.3.3 Area testing

Where as the previous testing was a rough estimate of the connectivity potential of the LoPy modules at ground-level, the second group of tests were conducted to more rigorously evaluate the connectivity potential. This was done by using the effective range determined in the previous tests to position more base stations in different locations to attempt to make any conclusions spatially independent although this

is something that was evaluated using the created predictive model. Below are two figures that visually explain the methodology of the area testing. In the first, the inner hex has a radius of the effective range found from the previous effective range testing which can be found in section 4.2.1. The outer hex has a radius of twice this effective range. This outer hex describes the range that will be tested for each testing location. The second figure describes how the testing range of each location will overlap with one another with the red effective range hex having a node at alternating corners of its hex resulting in every point in the red central hex having a measurement either on or near it with two base station locations within effective range and two or more in ineffective range.

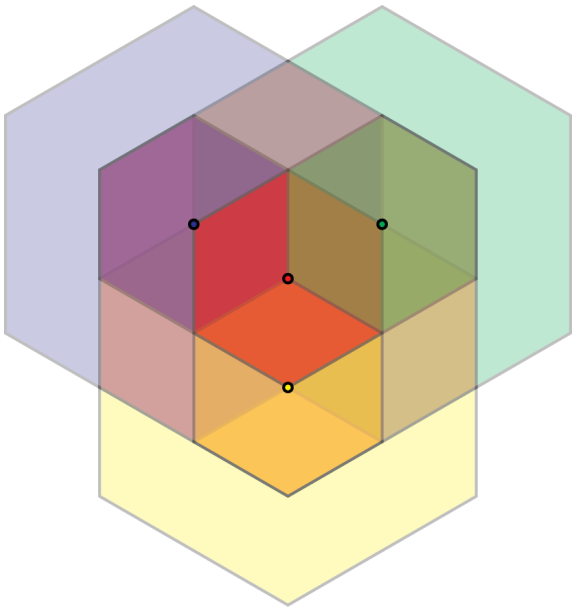

Figure 3.4: Area testing positioning template picture

This overlapping nature gives to an extent, a more spatially independent measure of how well the connectivity potential of a location is in the urban environment. If this is not the case, then the area tests should, at least, provide a good measure on how effects such as multi-path fading and shadowing effect the connectivity of the LoRa protocol and the LoPy modules. These tests will be run at three SF, 7, 9, and 11 at multiple different tests sites. This is done by deploying several base stations at once, two for SF 11, three for SF 9 and 4 for SF 7, allowing for greater efficiency in gathering test data since it will require fewer testing passes to gather the data. This is done by having the node ping all the base stations in the same fashion as the effective range testing which then replies in a staggered fashion with each packet labeled by the base station number to prevent crosstalk which is then received by the mobile node. The mobile node does this by listening for a certain length of time after pinging and recording all received packets in the time frame. If a reply from a base station is not recorded during the listening time frame, the packet is listed as a failed transmission. This results in a ping and a series of replies which includes the connectivity statistics of the ping in addition to the LoPy generating the connectivity statistics for each reply. The results are then sent to the laptop via

serial to be recorded in a CSV document for further analysis.

An important caveat of this testing is that certain testing locations may be impossible to place given that a building is in the way. This was an unavoidable obstacle that was compensated for by choosing the closest viable location to the ideal location. The paths where data was collected also stay primarily to roads or pedestrian paths in order to make data gathering as efficient as possible given the large measurement areas and a large number of tests.

Below are figures showing the testing locations and testing areas for each SF.

Figure 3.5: Area testing positioning SF 11

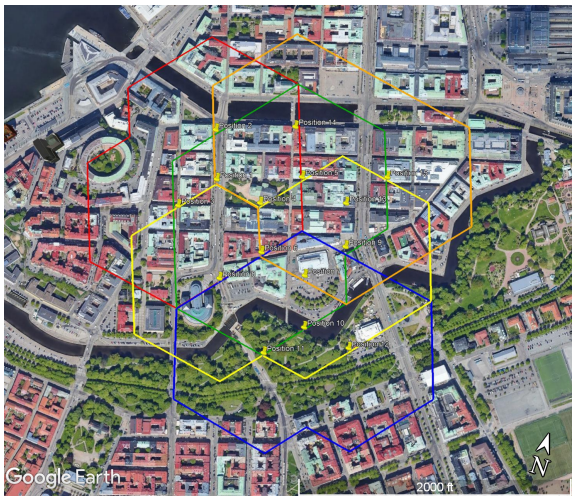

Figure 3.6: Area testing positioning SF 9

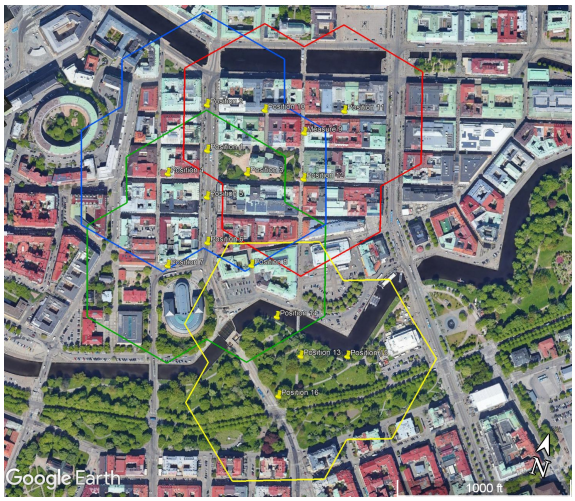

Figure 3.7: Area testing positioning SF 7

3.3.4 Location category tagging

The larger data set of the area testing, taken on its own, lacks the nuance and context of the testing methodology and may be of limited usefulness in actual deployments. However, gathering subsets of connectivity data points out of the larger set allows other perspectives to be looked at. This is done through picking data points from specific base station locations that have certain characteristics that may be seen in such a deployment. To accomplish this, several different scenarios were chosen that were both unique from each other and were shared by the area testing across all 3 tested SFs. These are listed and roughly defined below

- Alley - An environment formed by the two closest walls being 4 meters or less but less than a combined 15 meters from the sensor forming a corridor extending in one or both directions from the sensor or more than 15 meters.
- Road/Semi-Open Space - An environment formed by the closest two walls/-major obstacles being at least a combine 15 meters away from the sensor but less than 50 meters and forming a corridor that extends at least 50 meters in one or both directions. This should have the possibility and high likely hood of traffic in said environment.
- Park/Open Space - An environment lacking significant man-made structures in at least 2 directions of the sensor that would interfere with LoS communications

These location types are tags for the base stations and the sensors data is tagged with if the sensor had LoS or not. The area testing locations were chosen so that base station placement covered at least 3 instances of each or in other words, 3 locations in alleys, 3 locations in semi-open spaces, and 3 locations in open space. However it is important that certain scenarios will be a severe lack of information over certain distances given their description. An example of this is data gathered from a base station in an open space with the node in non-LoS being only viable from 80+ meters away due to the inherent nature of an open space having an open space surrounding it. These restrictions are shown in 3.3.3 and the appendix, along with the robustness of the measurements compared to other scenarios and distances. Additionally several

scenarios might lack data due to time and positioning restrictions on testing which will be discussed in 5.

3.4 Urban wireless connectivity data analysis

In order to draw meaningful conclusions from the data gathered, some statistical analysis was required. This analysis took the form of drawing out measures such as average received RSSI, rates of occurrence, and others listed below under 3.4.1 in addition to more spatial analyses in the form of heat maps and data points on maps. The goal of these measures is to confirm the veracity of the data gathered in addition to the viability of connectivity.

3.4.1 General data analysis

Analyzing the data set in its entirety and on a position-by-position basis allows more general conclusions to be gathered about the connectivity behavior in an urban setting more generally. This will be done using the techniques listed below, along with the presentation of the results of these techniques in 3.3.3.
However, several issues remain with the data gathered that need to be addressed. The primary issue with the data gathered in the tests is the unevenness of the sample distribution spatially. Certain locations have a larger number of samples due to the routes taken and overlapping or uneven speed in gathering the data. Several methods were devised to attempt to rectify this issue. The first is a strict moving average in multiple samples being closer than 5 meters from each other. The second is Spatial Gaussian Smoothing which attempted to smooth out potential data outliers by having averaging points taken at the midpoint between all samples as long as a minimum distance between each averaging point was 8 meters; otherwise the proposed averaging point was skipped. These averaging points then took into account every sample in a 10 meters radius and weighted them according to their distance between the sample and the averaging point based on a Gaussian window with sigma 1. The resulting sum was divided by the total sum of all the weights resulting in effectively a distance stepped Gaussian moving average over the data gathering route. Finally, for measures like outage rates, a moving average was taken similarly to the first method but in regards to the ratio of successful and failed messages.
With the spatial sampling discrepancies taken into account, various measures were compiled to give greater insight into conclusions that can be drawn from the data. These include the following.

- Outage Rate - Identify the outage rate at distances to highlight how reliable communication is.
- RSSI over distance - Used to understand how the signal strength varies over distance
- Number of Samples over distance - Used to gain an understanding for which distances were robustly measured

These measurements are presented in sections 4.3.3.1, 3.5.2, and the conclusions drawn are then discussed in 5.1.3. The metrics for evaluating the various scenarios

are the same as for the data more generally.

3.4.1.1 Heatmaps

As discussed in section 5.1.3, LoRa connectivity is inherently spatial in the sense that each location has unique connectivity characteristics both in terms of the spatial location itself but also the spatial location of the other node that a connection is being made too. This makes the generalization of this connectivity very difficult to accurately create and represent. However, this report makes an attempt to do this by using distance compensated, derived using the equation (3.1), RSSI results from 4 base station positions as described above in section 3.3.3 to show an averaged connectivity capability for several spatial points within the inner hexagons. While not ideal, this should present a more generalized view of the connectivity in different parts of an urban environment. Several heat maps are created, two for each SF. The first is based on the raw data and the second based on the Gaussian smoothed averaging as described earlier. This heatmap overlayed with blacked out regions for buildings should provide at least a somewhat generalized visual representation of connectivity in the urban environment.

3.5 Basic channel model

By taking the data from the previous testing with a special focus on the scenario testing, a path loss and outage model are created that help in predicting the potential connectivity of a sensor at a given position from another. This is done by assigning any potential base station and communications node with the distance between both sensors and the LoS is achieved by the placement. Using path loss models explained in section 2.6 created by the early testing data for the larger data set and each of the 2 LoS scenarios, the estimated path loss probability distribution and likely outage distribution will be presented. This model is based on comparatively basic communications theory since more advanced techniques would require either more sophisticated equipment or advanced modeling software with greater computational power. Some simple testing conducted in section 3.5.3 shows if the model was reasonable. As mentioned earlier, certain scenarios will lack significant data for certain distances impacting the model.

3.5.1 Path loss

The path loss model starts by estimating the loss in power in the received signal after traveling in traditional free space. This relationship is described in section 2.6. Given that the frequency being measured is $869.45MHz$, this leads to a wavelength of $0.33438m$. When these are placed into (2.11) leads to the equation (3.1) which describes the estimated path loss over distance for the LoRa packets.

$$P_{rdBm} = P_{tdBm} + 10log_{10}\left(\frac{G_l * \lambda^2}{(4 * \pi * d)^2}\right) \tag{3.1}$$

While the above works well in an open environment with no buildings or obstacles, the urban environment being studied has an abundance of buildings and obstacles which will lead to reflection, refraction, blockage, and scattering of the signal which will take the form of shadowing and multipath fading described in sections 2.6.2.4 and 2.6.2.3 respectively. Starting with the shadowing component, shown in equation (3.2), γ which is the path loss exponent and is used to approximate the average level of fading that occurs in the environment between the two points. This gamma is unique for each separate testing location and is roughly estimated as the mean value of the RSSI values from the sent packets while accounting for the outage rate of the communications link discussed in section 3.5.2 which brings the mean value down at longer ranges where there is a higher outage rate effectively hiding the lower RSSI results beneath the sensitivity of the sensor. Additionally, d_0, which serves as the reference distance is going to be set at 10 meters given the outdoor nature of the testing which will then replace the FSPL model with empirical testing so as to cover for constant discrepancies between the model and reality. Additionally, the potential antenna gain in the system and other losses of the system will be estimated at d_0 providing the constant K which represents most of the inherent standard gains and losses of the system such as antennas, cables, amplifiers, etc [30].

$$P_{r_{dBm}} = P_{t_{dBm}} + K_{dB} - 10 * \gamma * log_{10} * \left[\frac{d}{d_0}\right] \tag{3.2}$$

The results for both γ and K are shown in section 4.4. While the above equation does take into account shadowing, it fails to account for the environments non uniform nature. Shadowing at all positions will not be static and additionally, the behavior of the waves will also fluctuate in the environment even if the environment itself is completely static. These stochastic discrepancies will be covered with a random variable with a log-normal distribution as described in (2.6). As stated in section 2.6.2.4, the log-normal distribution covers the stochastic effects of shadowing fairly well. Since the gathered data is RSSI values which are a measure of signal power in decibels, the log-normal distribution must also be squared to account for this. This distribution is simply a Gaussian distribution as shown in 2.3. This distribution is defined below as X in 3.3 where the mean $\mu_{\phi_{dB}}$ is equal to zero as the average path loss is already taken into account by the path loss exponent in (3.2).

$$X_{\psi_{dB}} = p(\frac{P_{t_{dBm}}}{P_{r_{dBm}}} = \psi_{dB}) = \frac{1}{\sqrt{2\pi}\sigma_{\psi_{dB}}} \exp\left[-\frac{(\psi_{dB} - \mu_{\psi_{dB}})^2}{2 * \sigma^2_{\psi_{dB}}}\right] \tag{3.3}$$

Combining the distribution in (3.3) with the simple model yields the following equation:

$$P_{r_{dBm;X}} = P_{t_{dBm}} + K_{dB} - 10 * \gamma * log_{10} * \left[\frac{d}{d_0}\right] + X_{\psi_{dB}} \tag{3.4}$$

In addition to shadowing, the multipath impact is going to be taken into account. By taking (2.24) and adding it to the simple model, the RF behavior in urban Göteborg will have a modestly complete model.

$$Y_{Z^2} = \frac{1}{P_{r;X}} e^{-y/P_{r;X}} \tag{3.5}$$

This complete model is shown in (3.6).

$$P_{r_{dBm};X;Y} = P_{t_{dBm}} + K_{dB} - 10 * \gamma * log_{10} * \left[\frac{d}{d_0}\right] + X_{\psi_{dB}} + 10 * log_{10}(Y_{Z^2})) \quad (3.6)$$

This model is more suited for non-LoS signals given the use of Rayleigh fading as opposed to Rician, but it was decided to work only with Rayleigh given the ease of using the exponential distribution to model the power distribution of Rayleigh as opposed to integrating Rician fading which has no simple power distribution. Additionally, the environment was frequently highly trafficked which has a weakening impact on the LoS component of the signal making it reasonable to approximate fading with Rayleigh despite the LoS nature of parts of the testing. The model was fitted to all three SFs for both LoS points and non-LoS points given the large differences in outage rates and average RSSI values as shown in sections 4.3.3 and 4.3.3.1 respectively.

3.5.1.1 Monte Carlo modeling

Given the addition of a Gaussian distribution for the shadowing component of the complete model and an exponential distribution for the multipath component, Monte Carlo simulation was used to generate a rough approximation of the probability distributions for various distances. This was done by generating 1000 samples of the Gaussian distribution for each distance increment and subsequently generating 100 samples of the exponential distribution from each of the samples of the Gaussian distribution resulting 100000 samples per meter for each SF and the LoS and non-LoS cases. This number of samples was chosen as it was what the memory of the computer being used to run the simulation was capable of handling.

3.5.2 Outage rate

Given the real-world testing environment with the quality of equipment being used, the test data is naturally going to have failures. As seen in the LoRa modem chip set data sheet, signals are detectable to both a certain RSSI value and SNR value depending on SF. These are shown in table 3.1.

	RSSI Floor	SNR Floor
SF 7	-122	-7.5
SF 9	-128	-12.5
SF 11	-132	-17.5

Table 3.1: RSSI and SNR detection limits for LoRa modem

These hard limits mean that a part of the gathered data is effectively hidden making analysis and model fitting significantly more difficult since, for example, the true mean or standard deviation of the signal strength at a certain distance is hidden by the communications failure. Methods to compensate for this were used when fitting the shadowing distribution by estimating the mean of the received signal by setting

all failures to their minimum value and then deriving the mean. With this mean, the standard deviation was also estimated by censoring the data higher than the average and using said data to fit the shadowing distribution. This will result in a possible underestimation of the mean at high failure rates however given that the true mean could be below the hard limit but is 'hidden' by the failures. This fitting was done by using the Maximum Likelihood Estimate function in Matlab [15].

3.5.3 Testing soundness of the model and data gathered

The statistical models of the connectivity were checked for reasonableness by testing connectivity at each scenario at distances of 33% increments of the measured range if possible. At each of these locations, 100 measurements were taken and then compared to the statistical model and the area testing data gathered to see how well the average signal strength and outage rate compared. This was done by comparing the difference of the measured values to the distribution of the estimated values.

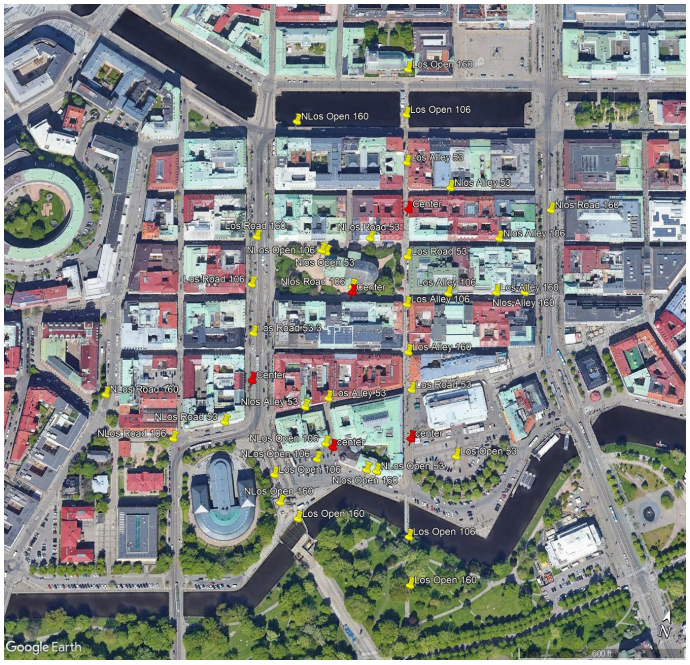

Figure 3.8: SF 7 P2P scenario testing points

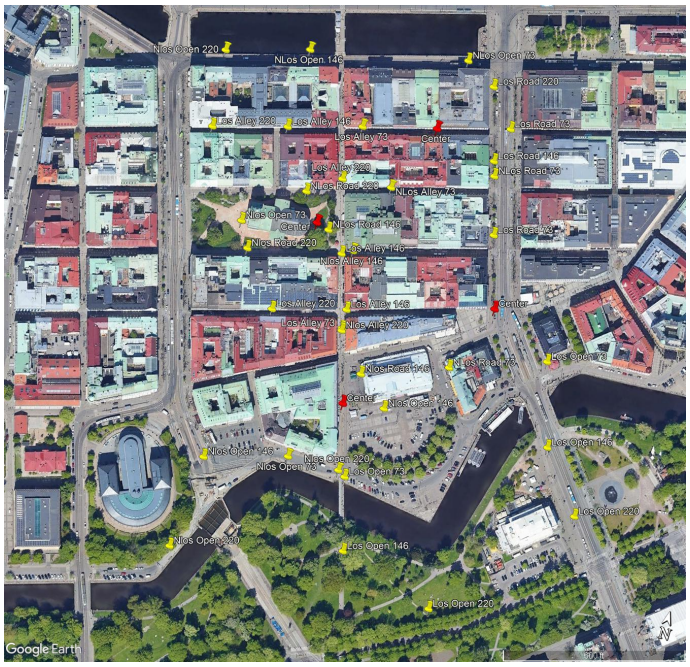

Figure 3.9: SF 9 P2P scenario testing points

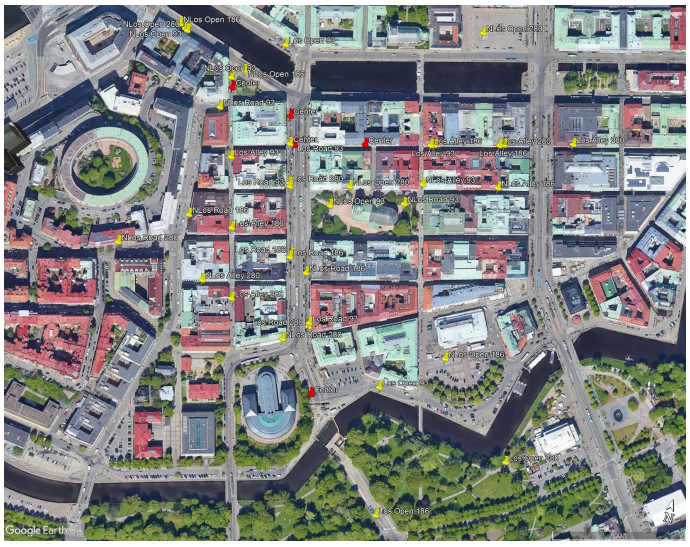

Figure 3.10: SF 11 P2P scenario testing points

3.6 Mesh network creation

The harsh RF environment in an urban location proposes a variety of challenges for a wireless network to operate efficiently, whether it be in signal blockage due to buildings creating shadowing and multipath effects or in the randomness in the behaviour of channel due to the continuous change in the surroundings like vehicular and human traffic. This makes it more difficult to predict and in return model a connectivity approach that fits a wireless sensor network application deployment in

a general setting. That is why the network should be equipped to compensate for the lack of an ideal connectivity environment by having various options functionalities to ensure a robust and efficient mode of operation.

Keeping those points in mind, the network was created with the intention of testing the advantages that a mesh approach could provide over a tree or star topologies to scenarios where IoT sensor applications could be required in an outdoor urban setting. All these criteria have helped set up the network's logical backbone and highlight the main deliverables when facing different trade-off decisions.

3.6.1 General architecture

The architectural structuring of the mesh sensor system was built to serve both personalized and industrial purpose networks that need to prioritize flexibility of adaptation, scalability of the network nodes and the ability to be deployed and left uninterrupted for a while which results in energy savings with the available time and resources provided.

Functionalities like the prior mentioned are to be added to the characteristic property of a mesh network which is the flow of information as per the networks need through different operational nodes in order to reach the sink for uplink. This leads to an architectural hierarchy of two layers, the lower being the sensor LoPy nodes, referred to as end-nodes, and the sink node operating as a gateway. The flow of data can occur throughout the different end-nodes at a given time in order to route the packet payload to the gateway node. Meaning that end-nodes also operate in relay mode, where when they are not sending data themselves, they act as a relay for other nodes which will be explained more in the 3.6.3 subsection. The gateway acts as a router where all the data converges and is sent to the application interface using a WiFi connection through Infotiv's Message Queuing Telemetry Transport (MQTT) broker.The gateway also does process on the network level, by keeping track of active nodes in the network and refines that list to provision or remove nodes based on their activity.

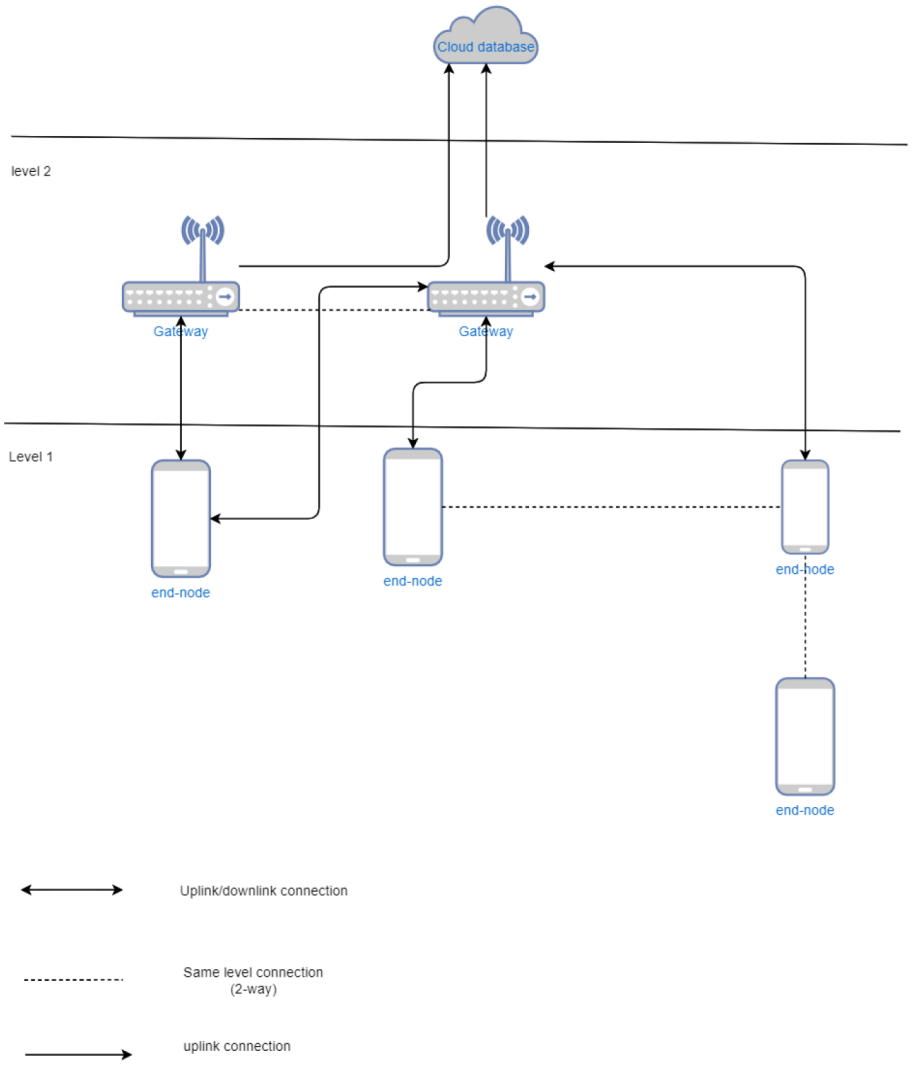

Figure 3.11: Mesh network architecture

This topology allows for nodes to act as routers to allow hopping of packets to reach the gateway increasing the effective range of the network with a comparatively small increase in latency time. This topology gives awareness to the end-nodes to adapt and maintain their routes to the gateway not only in case of a relay node failure, but also allowing for the end-node to be moved and deployed in another area of the network as they receive information about the positions of their neighbors, a property of mesh networks that is not present in LoRaWAN.

3.6.1.1 Routing protocol

The routing protocol was kept simplistic to manage the control traffic, which is the information that flows in the network necessary to configure and synchronize the network operation. A custom proactive routing approach was used, which meant that the nodes' route tables were updated in fixed intervals of time using beacons sent by the gateway. These network's "join" beacons are also relayed by the nodes, segregating them based on how many hop links they are away from the gateway

with a limit of 3 hops. This approach's advantage is on-demand sending with low latency but at the cost of increased network overhead while maintaining routing tables which adds to the complexity. A disadvantage of this custom protocol is the added constraint on node mobility, as node displacement cannot be more frequent than the route broadcast intervals.

3.6.1.2 Multiple access

An access scheme similar to that used in LoRaWAN, ALOHA, was implemented due to its simplicity and lack of added control traffic data. ALOHA protocol is simply the transmission of packets by nodes onto the network as soon as they are ready without inspecting the activity of the channel, that is, randomly. However, since the devices operate only on a single channel at a time, Time Division multiple access (TDMA) protocol was used to allow access to the shared channel. Additionally, slotted ALOHA was implemented where nodes selected a random time slot to transmit on and after sending wait for an acknowledgment to validate the packet or retry transmitting within the same time slot if no acknowledgment was received. The time slots were divided based on airtime calculation to include the round-trip journey with accommodation for re-transmissions if needed. In terms of addressing between nodes, the messages shared are either Unicast or a broadcast, multicast addressing is not available using the custom mesh network.

The vulnerabilities of this approach lie in the probability of collision, that is,if two nodes pick the same time slot to send randomly which will cause either one or both packets to not reach the sink. The calculations for probability of collision throughout the retries is mentioned in 3.7.1.

3.6.1.3 Mesh protocol

In order for the network to operate with the least amount of intervention, self-stabilizing route maintenance was applied through fault-tolerant algorithms. If a node in the network were to fail for any reason, the rest of the network tries to readjust and another node will take the relaying responsibilities. This takes place during the periodic beaconing cycles sent out by the gateway for the nodes to map out a surrounding neighbor to relay it to if that end-node is not in the direct vicinity of the gateway which allows for mobility. End-nodes store only the path necessary to reach the gate minimizing memory and control traffic needed to keep the network functional.The features of route discovery and maintenance in a mesh network is one of the major differences to star topologies adaptations.

While the nodes handle the routing, the gateway acts as a server as well in provisioning new nodes to the network by sending out join broadcasts which allow for new nodes to join and also synchronizes the timing cycles between the end-nodes and the gateway. The gateway is also responsible for keeping track of inactive nodes (i.e., fail to send an uplink) and if they exceed a certain amount of time without any activity the gateway deletes those node entries and they would have to attempt to rejoin the network again.

3.6.2 Packet construction

The packets were designed to carry the lowest load possible of control traffic to reduce the size of each transmission. By having the gateway perform the server roles of provisioning/removing nodes, headers to map the packet to application level were not needed. Three packets are mainly used for the flow of data in the network.

- **Data packet:** Consisted of 6 headers, each 1 byte in size. While the payload can be of variable size to adapt to different kinds of messages depending on the application being used. The first header contained the **sender device** randomly generated ID in hexadecimal. This was meant for allowing the receiver node to register and save the origin of the packet for acknowledgment sending or relaying. **Length of the packet** is the second header introduced to give the LoPy what to expect for the variable payload length and to prevent attacks by sending long payloads to slow the network down. **Hop number** is the third header in the packet to account for the number of hops made by the packet already influencing the decision whether to relay the packet or not depending on if it reached the maximum hopping limit. **Destination ID** is meant for designated addressing to help navigate the packet in the network. **The relay node** is also used for addressing for the node to be aware of the path the packet has taken. And the sixth header would be **payload stat** which is a hexadecimal number decided on beforehand to indicate the type of packet and prevent tampering with the packet.

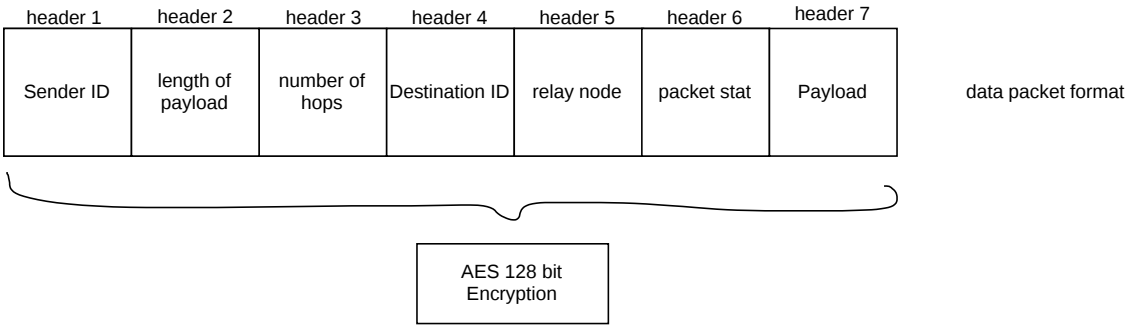

Figure 3.12: Data packet format

- **Join packet:** It consists of 5 headers, 1 byte each. The first header was sender ID to recognize the origin of the packet which is critical for the mapping out the location of the node with respect to the neighboring nodes. Hops is also part of the join packet as this is also relayed based on the number of hops.

Broadcast number is the third header which tracks the number of broadcast packets sent which is critical for provisioning and synchronizing new nodes into the network. The previous node is to indicate the path of the beacon if it was relayed from an end-node or received from the gateway. The last header is a join packet stat to keep ensure the integrity of the broadcast.

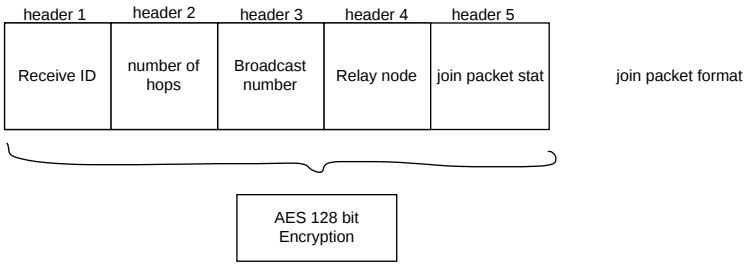

Figure 3.13: Join packet format

- **Acknowledgment packet:** A small packet of two headers to indicate the sender ID and the acknowledgment stat for ensuring the validity of the packet.

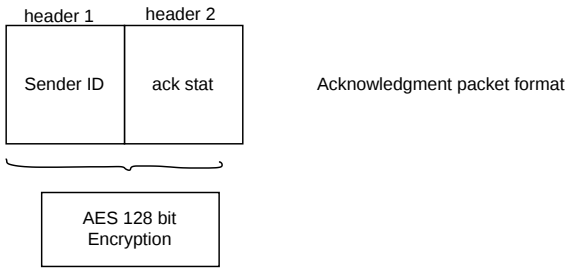

Figure 3.14: Acknowledgment packet format

3.6.3 Modes of operation

The flow charts in figures 3.15 and 3.16 explain how the end and gateway nodes operate and the different functions carried out.

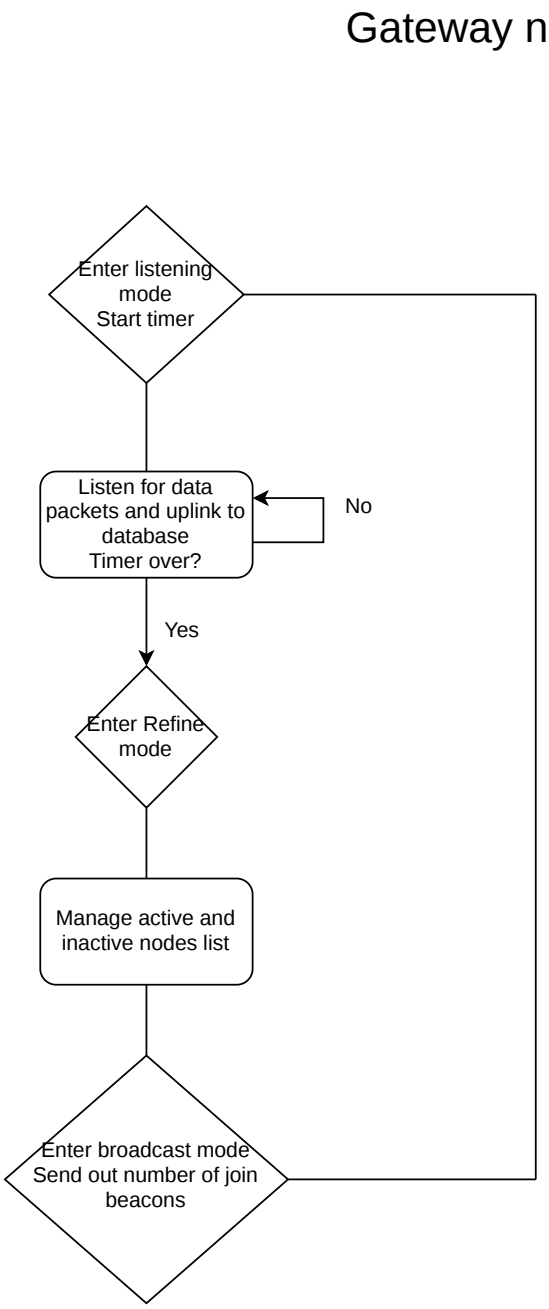

Figure 3.15: Gateway node code flowchart

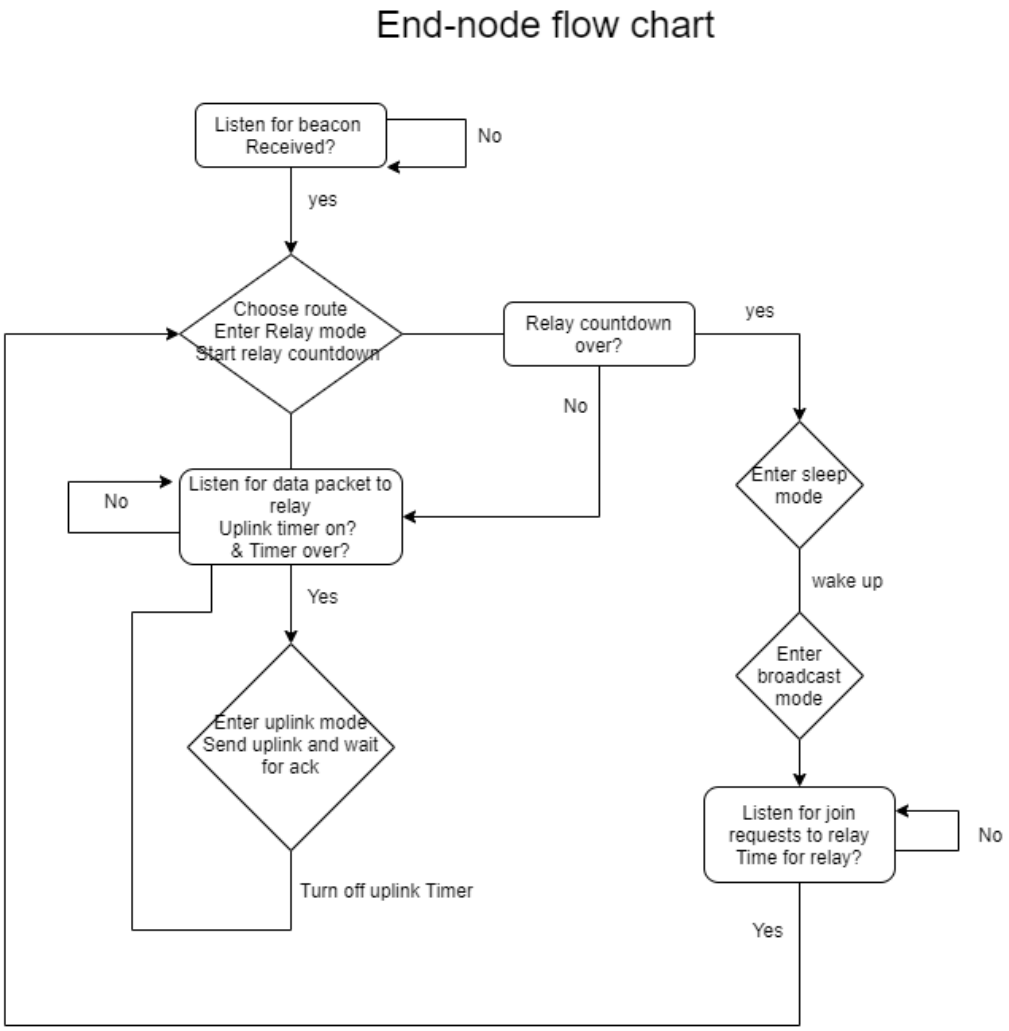

Figure 3.16: End-node code flowchart

3.7 Network evaluation

To evaluate the performance and successes versus failures of trying to implement a LoRa mesh network, several metrics needed to be measured. These metrics, together with the results from the area testing should give an answer to whether the criteria set out at the beginning of this report have been achieved or not. A list of these metrics and their contribution follows below.

- Data Rate
- Network Creation Time
- Node provisioning Time
- Number of node hops
- Latency
- Outage Rate
- Range
- Security

The mesh network parameters were designed around permitting an extended range of connectivity for LoRaWAN operation by adopting a **decentralized network topology**. Hopping between was limited to 3 hops to prevent the increased delay in message reception while also providing a range of more than 300 meters with measured node deployment. It is important to note that range calculations were influenced by the fact that a block's or a building compound's dimensions in the area tested in central Gothenburg do not exceed 100m * 175m. Another design metric was **acknowledgment** introduction for the reliability of message transmission and as a network operation diagnosis tool. Ack replies were coded to confirm the first hop from an uplink only and not throughout the network to avoid over-flooding the network and decrease latency.
To allow for **node mobility**, the degree of mobility was firstly defined. Since mesh routing depends on the node positioning to relay the packets to the gateway, mobility was limited to node replacement. That is, a node's deployment position can be changed at any time without any need for extra configuration as long as it is in range with another network node. This feature is supported by the characteristic function of the gateway to issue **route reconstruction** packets every broadcasting cycle. This also determined the **node provisioning time** by controlling other variables like node sleep time and length of listening and uploading cycles.
Energy consumption was not considered as a constraint during the network design process.

3.7.1 Custom mesh network in numbers

Metrics	**Expected Network Performance**
Frequency	869.4 MHz
Bandwidth	250 kHz
Data Rate	3.5 kbps
Network header size	6 bytes
Max. Latency	1.9 seconds (2.4 s for 3 hops)
Number of hops	2 (can extend to 3)
Network Creation time	50 $\text{seconds}_{1}*$
Network Capacity	80 nodes
Range	110 meters per $\text{hop}_{2}*$
Max. Node Provisioning time	1800 $\text{seconds}_{3}*$
Avg. Battery consumption	$50\text{mA}_{4}*$

Table 3.2: Custom mesh network metrics

The following are the metrics table footnotes.
1: Network creation times can be changed by controlling the number of broadcast messages sent by the gateway.*
2: The range of connectivity is very situation dependent and thus values may vary depending on LOS.*

3: Node provisioning time is decided based on controlling the how many readings would the nodes uplink.*
4: The average energy consumed when LoPy is idle. Goes to 92.6mA while transmitting or receiving per documentation [39].*

3.7.2 Outdoor urban testing

As the results of the Area testing show, positioning is a critical aspect of the viability of such a network. A test was designed to be performed to compare the capabilities of the two types of networks. It was to be a random spread of sensors in an area decided by using a random number generator in Matlab providing latitude and longitude coordinates in an area. If a location is inaccessible to the network, then the sensor will be placed at the nearest possible location. The area will be roughly a square kilometer in the area centered around position 1 in the area tests. The data sink's position factor will be tested in 2 different locations in the network. This should evaluate the mesh network's multi-hop capability to a limited degree and its effect on network performance as compared to the LoRaWAN's centralized type of network.

3.7.2.1 LoRaWAN vs custom mesh

The positions of the nodes generated within central Gothenburg were labeled 1 to 6 with one of the nodes set up as a gateway like in the figure above. It was important to have diverse deployment locations characteristics, which means that signals transmitted from the node should spread about in areas like alleys, open-spaces and roads to be able to compare the individual node results as well as the overall network performance compared to our earlier connectivity tests. The uplink timings were adjusted on the LoRaWAN nodes to match the rate of the custom mesh nodes.

For LoRaWAN network, the devices were configured and provisioned to 'the things network' by setting up the nano-gateway first. Since LoRaWAN adopts a centralized topology, nodes that were out of range of the gateway or surrounded by obstacles (buildings mainly) were expected to perform poorly considered their inability to route packets.
The setup was simpler in the custom mesh because the nodes in a mesh setup are self-configurable, so it was a matter of placing the devices in the respective locations and record the packets from the gateway.

4

Results

This chapter details the tests conducted and their results along with any data analysis from said results.

4.1 LoRa protocol

The physical layer parameters used for LoRa transmissions between nodes for the data gathering process were **spectrum** used was 869.4 MHz, **transmission power** used was the default LoPy setting for 14 dBm with a maximum packet size of 50 bytes during various tests. The recorded **RSSI** values for **1 meter and 10 meters** packet transmissions of 10 bytes in the open air were -49.7 and -70.7 respectively averaged over 1000 samples using SF 7.

4.1.1 SDR frequency spectrum and spectrogram

SDR results for noise or interference at frequency band based on 3.1 and spectrogram for LoRa packages at various SFs.

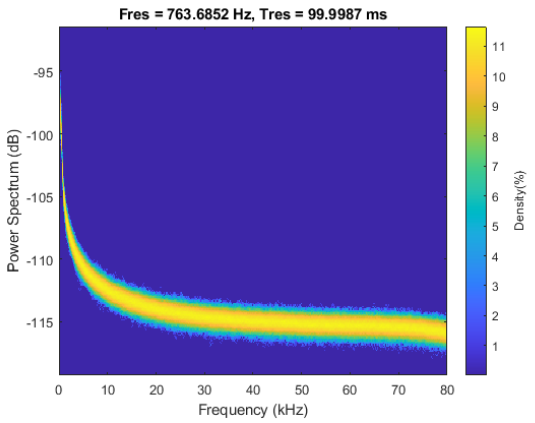

Figure 4.1: Frequency spectrum of noise floor at 869.45 MHz to 868.5 MHz using a persistent hold to identify any possible transients due to interference

The spectrogram gives a good view of how the LoRa packet is structured in both the time and frequency domains where it is clear how the data is encoded on the chirps. The beginning of the packet has the pilot chirps which is formed by 10 up chirps and 2 down chirps which are used for detection and synchronization.

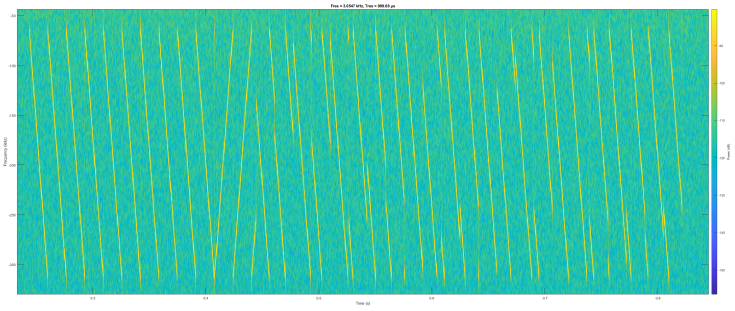

Figure 4.2: Spectrogram of a data packet transmitted at SF 11 with the frequency domain being flipped

4.2 Urban connectivity

To analyze the urban connectivity behavior, multiple testing stages were set to build a robust methodology approach to understand how the environment poses a challenge for the connectivity metrics of a sensor node network deployed at ground-level utilizing the LoPy's. The tests were divided into stages where the approximate P2P effective range was determined for different SFs, followed by area coverage testing by setting up multiple base stations in hexagonal cells to provide redundancy location independent coverage map.

4.2.1 Effective range testing

Effective Range testing results conducted for SFs 7, 9, and 11.

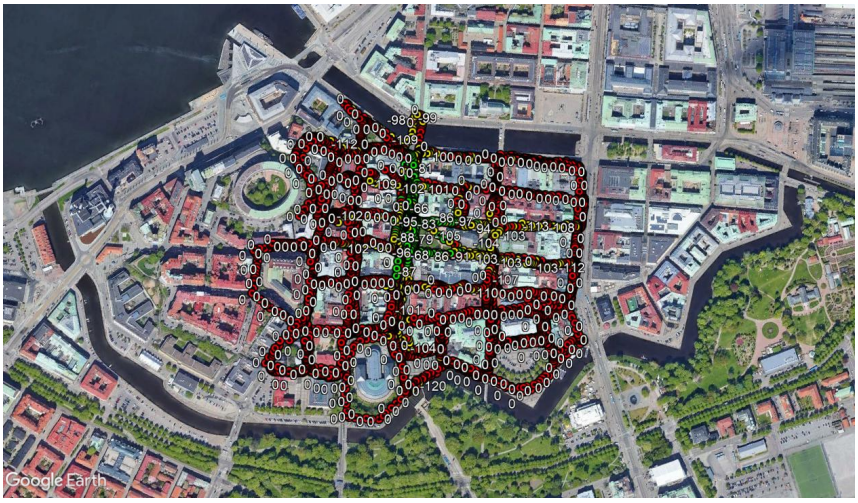

Figure 4.3: Effective range test data points SF 7

Figure 4.4: Effective range test data points SF 9

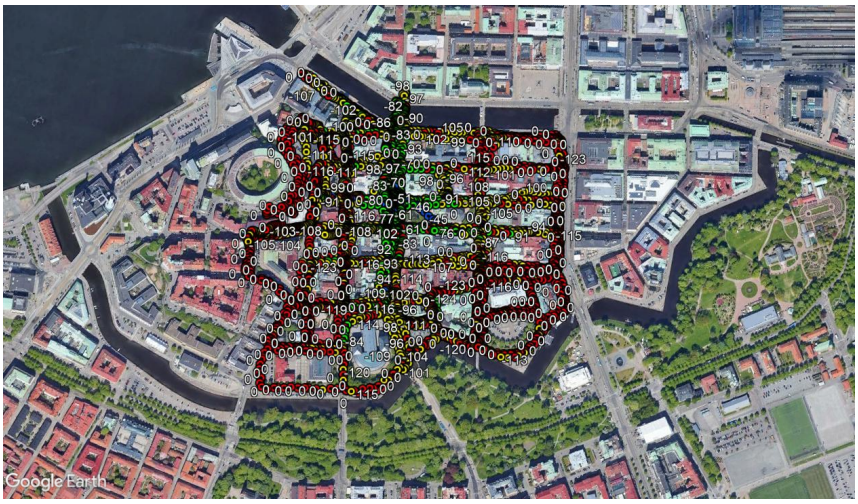

Figure 4.5: Effective range test data points SF 11

4.2.1.1 Outage rate

Outage Rate graphs for determining effective range at 80% packet success rate as a threshold for network operation.

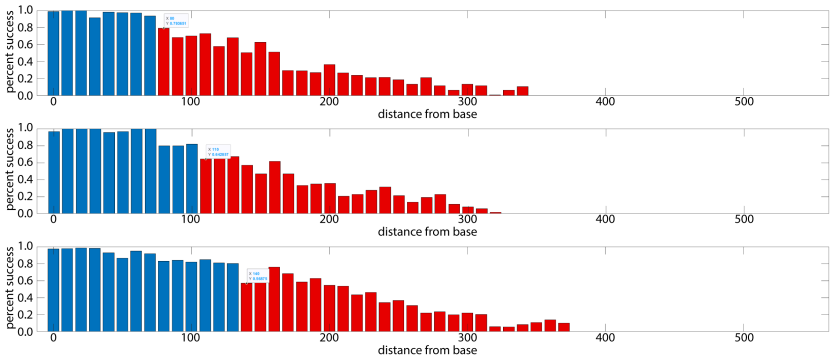

Figure 4.6: Outage rates at SF 7 ,9, and 11 with blue columns having a packet success rate above 80% and red columns have a packet success rate below 80%

The thresholds were 80 meters for SF 7, 110 meters at SF 9 and 140 meters at SF11.

4.3 Area testing

Area test results were conducted by dividing the location into hexagonal cells covered by the pinging base stations like in figure 3.6, where the pins represented the positions of the base stations. This section will provide the outage rate and RSSI graphs resulting from the area connectivity test of the three measured SFs followed by the scenario testing figures of area categorization, tags and positions of P2P tests along with featuring some interesting cases.

4.3.1 Map of data points

Pictures of Google Earth data sets showing data gathered during the entire area testing and for several handpicked positions.

Figure 4.7: Area testing data points for SF 11; data point color is irrelevant

Figure 4.8: Area testing data points for SF 9; data point color is irrelevant

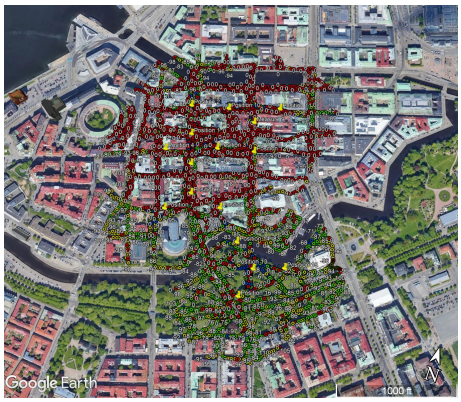

Figure 4.9: Area testing data points for SF 7; data point color is irrelevant

For pictures showing the data for handpicked positions the various colors are shown to mean the following: Red is a failure, Orange is for power less than -110 RSSI, Yellow is less than -90, Green is less than -70 and Blue indicates the rest of the RSSI values.

Figure 4.10: Area testing data points for position 1 with base station in a semi-open setting

Figure 4.11: Area testing data points for position 11 with a base station in an open setting

Figure 4.12: Area testing data points for position 5 with a base station in an alley/closed setting

4.3.2 Sample numbers

The figure below shows the number of samples that gathered for both raw data and the number of Gaussian averaged points for area testing as a whole, and also subcategorized for LoS data points and non-LoS data points. This is important to show the merit in the conclusions drawn from said data.

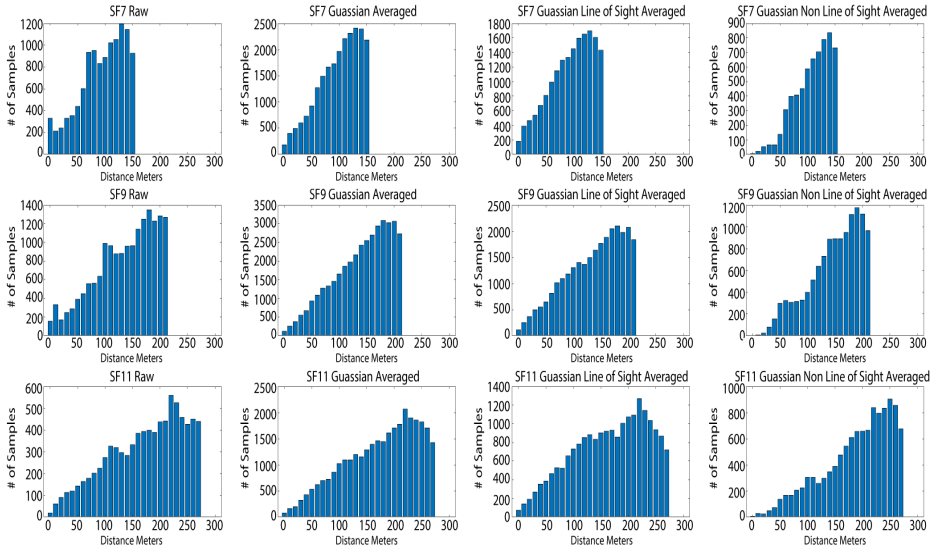

Figure 4.13: Number of samples

4.3.3 Outage rate

Various outage results for the overall area connectivity data gathered showing raw data, averaged and divided into LoS and non-LoS respective graphs for SFs 7,9, and 11.

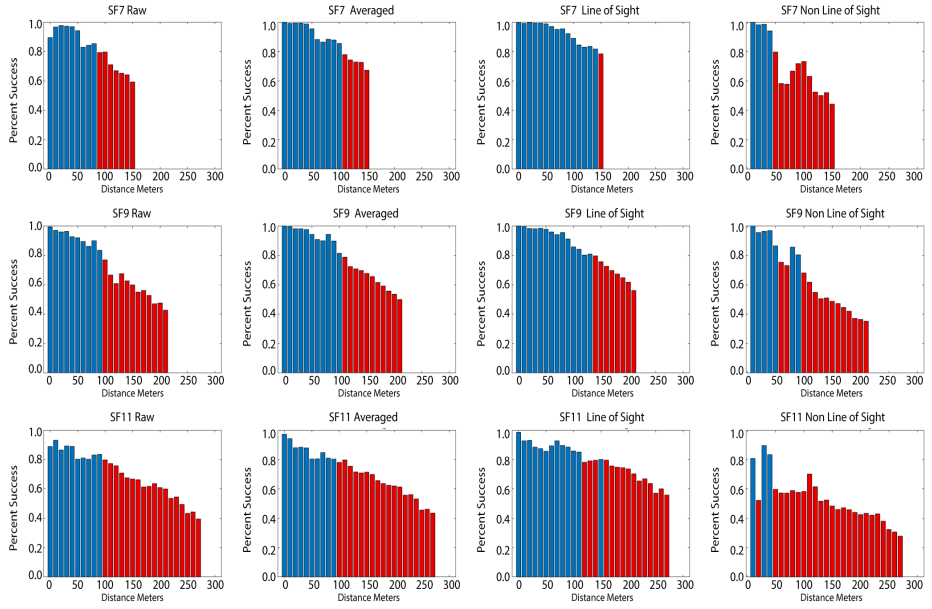

Figure 4.14: Area testing outage rates SF 7,9, and 11

Each position also has individual outage rate graphs in the appendix.

4.3.3.1 Statistics

RSSI statistics gathered from the area connectivity tests representing raw packet data, averaged and divided between LoS and non-LOS. Also, an RSSI scatterplot with a similar categorization is included.

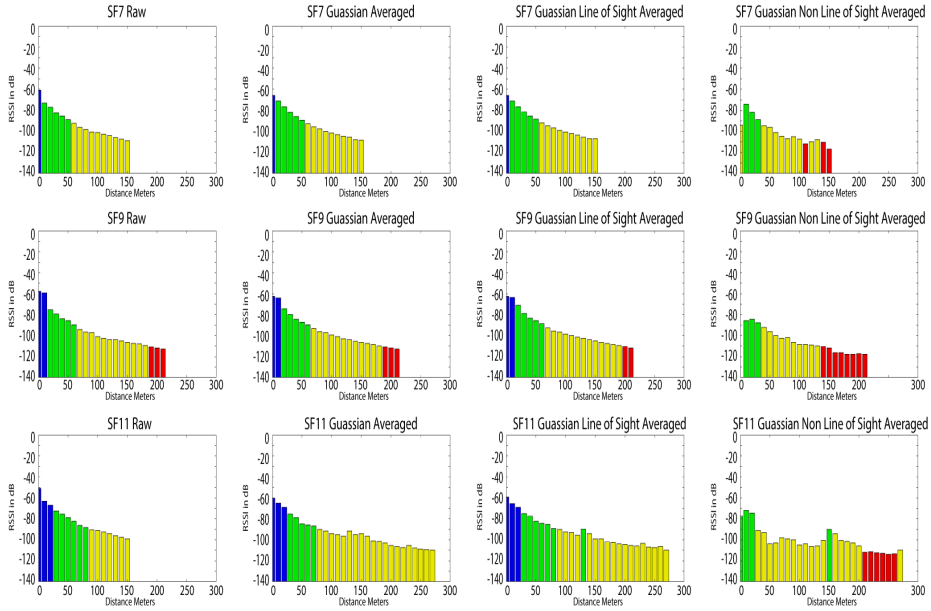

Figure 4.15: RSSI over distance

Each position also has individual RSSI average graphs in the appendix.

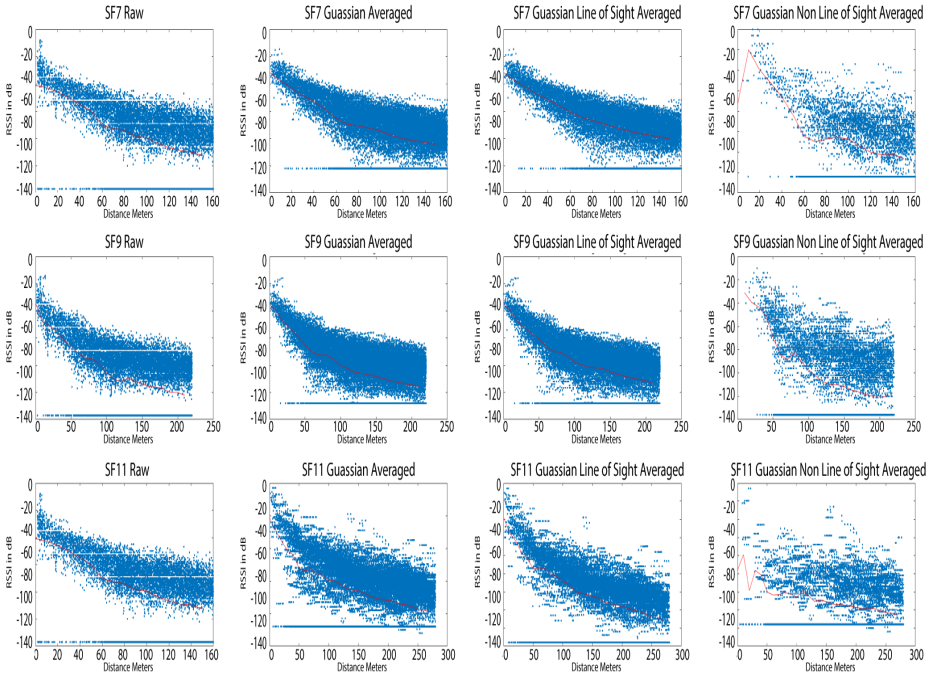

Figure 4.16: RSSI scatterplot

Each position also has individual RSSI average scatterplots in the appendix.

4.3.3.2 Heatmaps

The following are the smoothed connectivity heatmaps for SFs 7, 9, and 11 constructed using redundant RSSI values from at least 4 base stations per location and corrected for propagation losses.

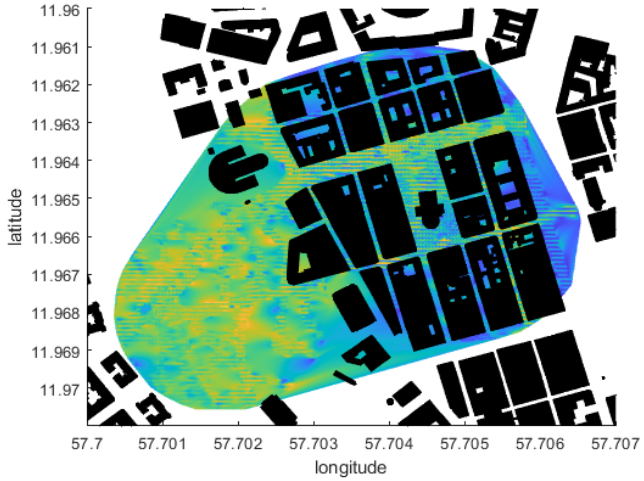

Figure 4.17: Smoothed heatmap SF 7

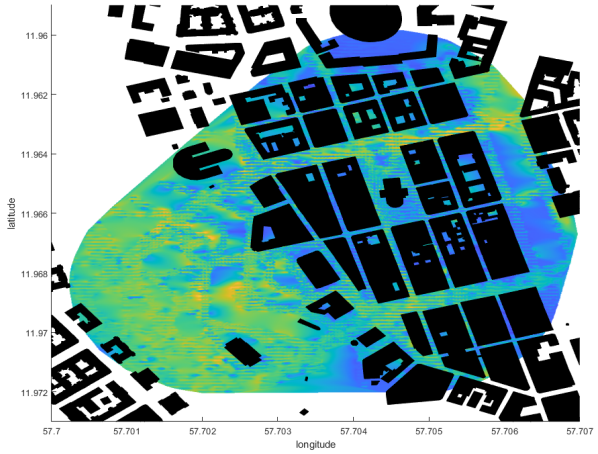

Figure 4.18: Smoothed heatmap SF 9

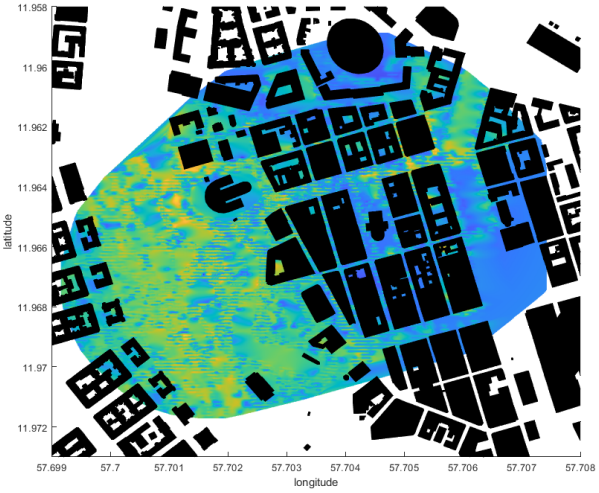

Figure 4.19: Smoothed heatmap SF 11

4.3.4 Scenarios

The area further divided into sections and scenarios where individual cases were tested and produced the following results.

4.3.4.1 Scenario demarcation

Colorization of the location to categorize it into 3 distinct scenarios, alleys in grey, roads in black and clear to indicate open spaces.

Figure 4.20: Scenarios defined

4.3.5 Scenario testing data

The below table presents a sample of the P2P scenario tests conducted by showing the packet success rate and RSSI average and variance values.

Location_distance_location_sight	Outage rate	Average RSSI	RSSI variance
Alley_73_Alley_LOS	0.950	-87.457	93.695
Alley_73_Alley_NLOS	0	-128	0
Alley_73_Open_LOS	1	-85.284	4.370
Alley_73_Open_NLOS	0.136	-123.20	15.528
Alley_73_Road_LOS	0.989	-87.342	25.845
Alley_73_Road_NLOS	0.837	-107.657	63.612
Alley_146_Alley_LOS	1	-99.460	6.822
Alley_146_Alley_NLOS	0	-128	0
Alley_146_Open_LOS	0.988	-98.100	15.069
Alley_146_Open_NLOS	0	-128	0
Alley_146_Road_LOS	0.988	-93.062	18.036
Alley_146_Road_NLOS	0	-128	0
Alley_220_Alley_LOS	0.989	-108.866	8.114
Alley_220_Alley_NLOS	0	-128	0
Alley_220_Open_LOS	0.95	-107.902	32.136
Alley_220_Open_NLOS	0	-128	0
Alley_220_Road_LOS	0.976	-99.293	30.070
Alley_220_Road_NLOS	0	-128	0
Open_73_Open_LOS	0.976	-86.203	44.300
Open_73_Open_NLOS	0.963	-106.063	21.986
Open_73_Road_LOS	0.914	-92.626	106.678
Open_73_Road_NLOS	1	-99.753	4.561
Open_146_Open_LOS	0.964	-101.549	35.628
Open_146_Open_NLOS	0.926	-112.0123	25.094
Open_146_Road_LOS	0.886	-96.513	111.377
Open_146_Road_NLOS	0.054	-122.860	13.725
Open_220_Open_LOS	0.988	-99.936	20.35
Open_220_Open_NLOS	0.145	-126.091	5.716
Open_220_Road_LOS	0.452	-109.365	116.738
Open_220_Road_NLOS	0	-128	0
Road_73_Road_LOS	0.988	-77.023	32.614
Road_73_Road_NLOS	0.976	-88.957	37.686
Road_146_Road_LOS	0.75	-99.703	159.329
Road_146_Road_NLOS	0.848	-105.031	73.579
Road_220_Road_LOS	0.913	-100.135	67.171
Road_220_Road_NLOS	0	-128	0

Table 4.1: A sample of individual scenario test data for SF 9

4.4 Basic connectivity model

The γ and values used in the model are shown in the table 4.2. The K value was determined to be -80.68 given the measured power of -60.683 dBm RSSI at 10 meters.

γ	LOS	non LOS
SF 7	2.684	4.384
SF 9	3.515	4.818
SF 11	3.600	5.552

Table 4.2: The gamma values table

The shadowing variable Gaussian distribution that was fitted to the data has criteria μ and σ which are presented in the appendix in a table. They were fitted according to the method stated in 2.12 and 3.5.2.

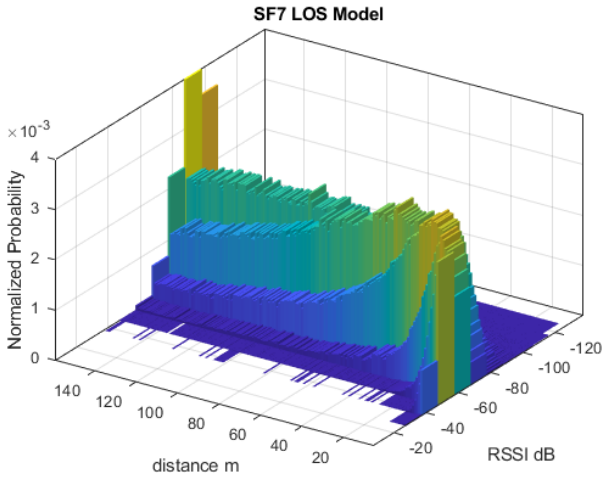

Figure 4.21: SF 7 LOS distribution model

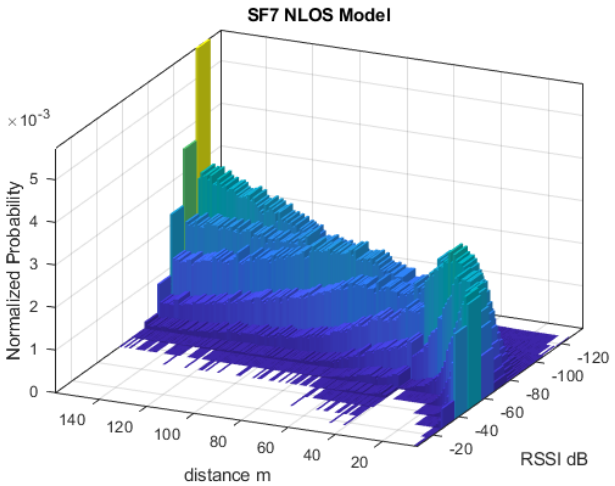

Figure 4.22: SF 7 NLOS distribution model

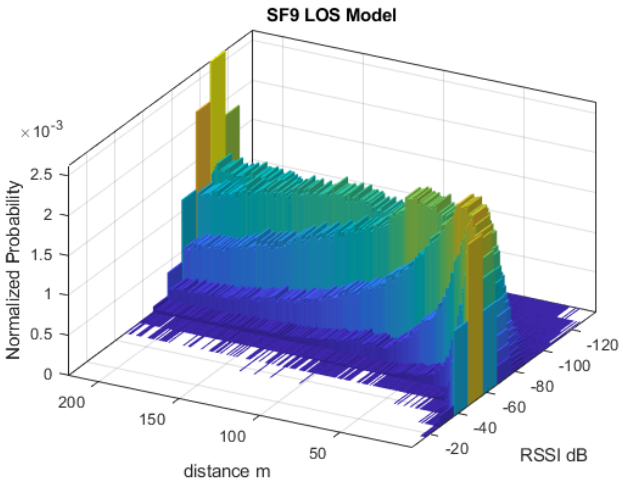

Figure 4.23: SF 9 LOS distribution model

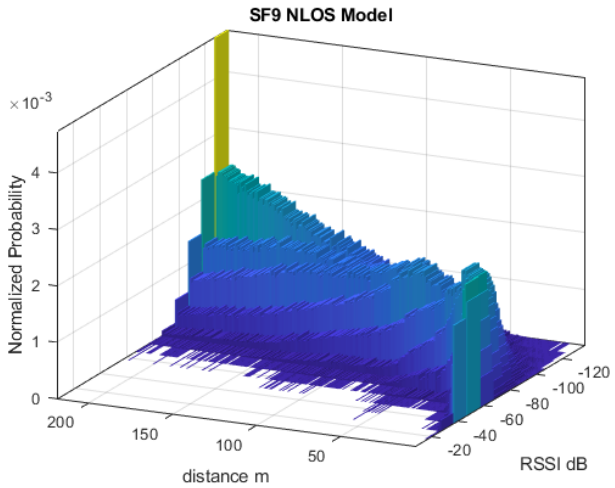

Figure 4.24: SF 9 NLOS distribution model

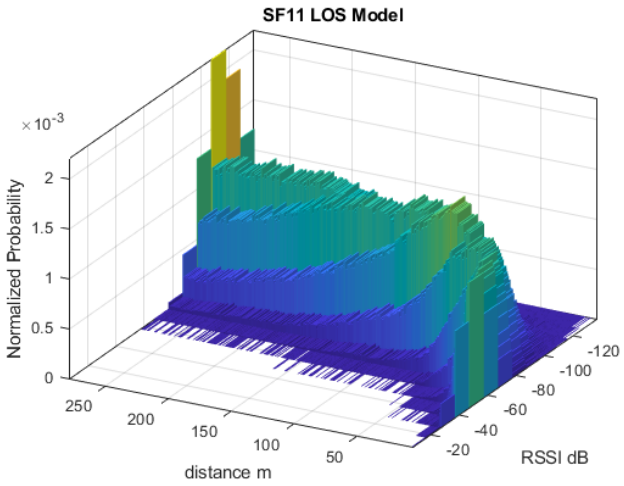

Figure 4.25: SF 11 LOS distribution model

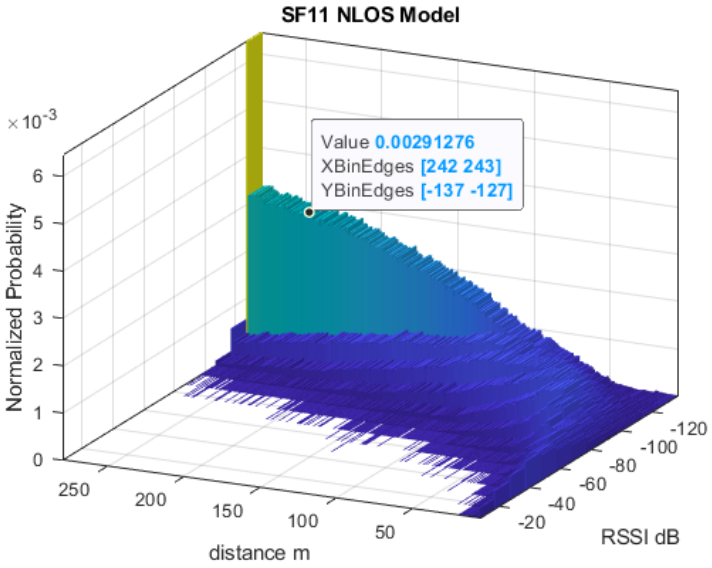

Figure 4.26: SF 11 NLOS distribution model

4.5 Network testing

Network Testing results for both LoRaWAN and custom mesh implementation in a random deployment scenario in central Gothenburg using 5 network nodes and 1 gateway.

Figure 4.27: Map of nodes' positions

Testing results for when nodes are placed randomly through Matlab generated latitude and longitude points named 1 to 6, including the gateway, deployed in a static scenario with interchanging the placement of the gateway between positions 6 and 5 respectively to inspect the adaptation of the custom mesh network in different geographical topologies while recording the success rate of 50 packet transmissions per node.

Test location 1	**Device 1**	**Device 2**	**Device 3**	**Device 4**	**Device 5**	**Total**
Mesh packets	48/50	35/50	40/50	46/50	39/50	83.2%
LoRaWAN packets	50/50	17/50	0/50	4/50	18/50	35.6%

Table 4.3: Mesh vs LoRaWAN outdoor network test-gateway at position 6

Test location 2	**Device 1**	**Device 2**	**Device 3**	**Device 4**	**Device 6**	**Total**
Mesh packets	49/50	43/50	50/50	44/50	47/50	93.2%
LoRaWAN packets	47/50	44/50	50/50	0/50	30/50	68.4%

Table 4.4: Mesh vs LoRaWAN outdoor network test-gateway at position 5

5
Discussion

This section interprets the test results and their portrayal of the wireless sensor system performance and discuss the effectiveness of the chosen communication method, network protocols and the resulting model along with arguing the validity of the adopted testing methodologies.

5.1 Urban environment study

The urban environment, from an RF perspective, can be seen as a channel with a set of challenges for a wireless network. The harshness of the RF environment deteriorating the signals is intensified by the introduction of a degree of unpredictability because of the continued changing of factors affecting the signals' propagation like multipath fading, weather conditions and traffic like cars, trams, trucks, construction, etc. Therefore, when trying to analyze ground-level connectivity performance metrics to judge the operation of wireless sensor networks using LoRa in central Gothenburg, the shadowing fade and LoS obstacles will be regarded most detrimental to the system from an RF stand-point as multipath effects are less impactful due to the comparatively long symbol time in LoRa chirps over a coherent channel as discussed in 2.6.2.3 [2].
Path loss calculations would be complicated if a pure analytical approach was used in this scenario due to the large number of factors contributing to the degradation of the propagating signal like diffraction, reflection, absorption, and multipath fading in a dense urban environment. Thus, to predict path loss approximation within an acceptable margin for short links (like those used in sensor networks), an empirical approach was used to examine the effect of urban channel on such deployments in central Gothenburg with an attempt to generalize the model. This is similar to methods adopted for cellular network modeling [41].

5.1.1 LoS vs Non-LoS: shadowing & multipath

The testing area was divided into two categories depending on whether the node had a LoS path to the gateway or not. It is important to note that LoS between nodes was assumed if the two devices had a direct line connecting them with no building obstacles in the way. However, realistically, some positions cannot be considered full LoS due to the geographic topology of the area with small hills obstructing signal paths or other numerous obstacles such as vehicles, fences, trees, etc. that would help prevent a full LoS from being achieved. With 80% set as the minimum for

package success rate for efficient network operation, the range tests were conducted to get an estimation of the ground performance metrics of the nodes.
Those range of suggestive values were used for area connectivity testing to obtain power received at certain distances and use those values to depict the location-specific outage rates.
Looking at a few samples of the area connectivity tests, for example, positions 1 and 6 in the following figures, show the benefit of such categorization where strong to bad RSSI values are depicted in blue with the transition scaling respectively from green to yellow to eventually red signaling failed transmission.

Figure 5.1: RSSI values spatial weighted averaging in SF 9 area test: base station position 1

Figure 5.2: RSSI values spatial weighted averaging in SF 9 area test: base station position 6

In the figure below, the laid over topography is the central Gothenburg area tested around with the latitude and longitude coordinates on the y and x-axis respectively. The areas of most favorable connectivity conditions as measured using LoRa signal of SF 9 are highlighted in yellow hews in the heatmap and can be easily seen how they are more prominent in open spaces and long roads where LoS can be established. More difficult locations are highlighted in darker blue. The heatmaps generated used distance compensated RSSI measures to reflect the environment's effect on path loss. In the area covered and demonstrated in the heatmap, at least 4 different gateway positions were used to provide coverage redundancy to ensure that the heat reflected nodes' reception quality in that certain position with decreased reliance on the gateway's position.

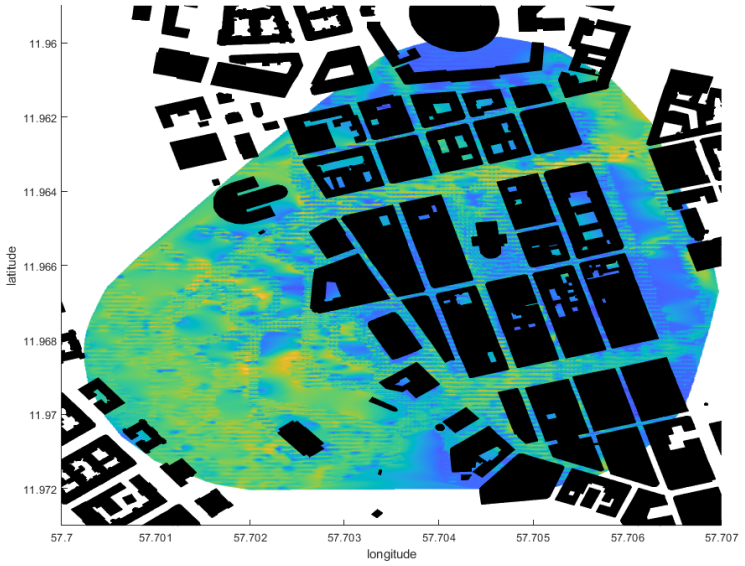

Figure 5.3: Heatmap for central Gothenburg in SF 9

After general area testing, in an attempt to generalize the model for similar locations within urban Gothenburg and also to get a more detailed insight on the extent of signal fading in specific sites, locations were further categorized into alleys, roads and parks to represent the different kinds of spaces for a node to be deployed in. Specific location tests were conducted to understand how a node placed in an alley would react with a node placed in a 'road' location but in those tests, not enough data could be collected overall to avoid outliers and give a robust conclusion, especially at smaller distances for non-LoS condition as we can see from the averaged sample distribution in figure 5.4. This makes sense given the lack of small buildings to provide the LoS obstacles for smaller distances. This could have been artificially done by introducing a conductive barrier between the nodes, but this brings other potential issues and was outside of the scope for the testing.

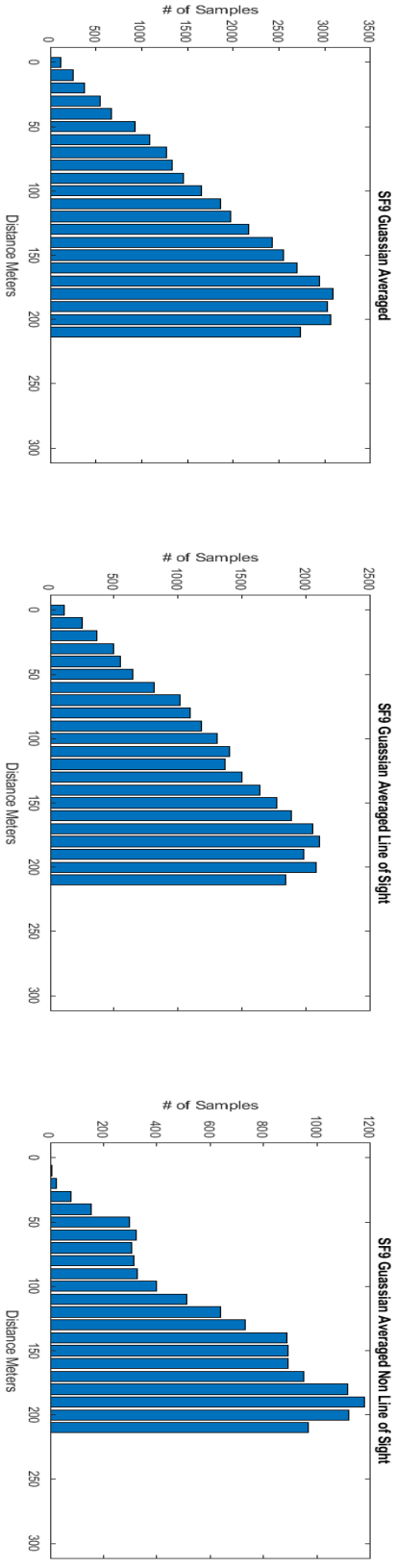

Figure 5.4: SF 9 data sample distribution

But what was apparent throughout the data, the shadowing margin (for non-LoS) plus the multipath effect appearing beyond close range, which was $\approx$ 40 m, the packet success rate becomes unguaranteed. This can be seen in comparing the outage rates of LoS and non-LOS conditions. This expected and more theoretically fitting path loss in RSSI can as well be seen in LOS readings while gets more chaotic in larger distances in non-LoS.

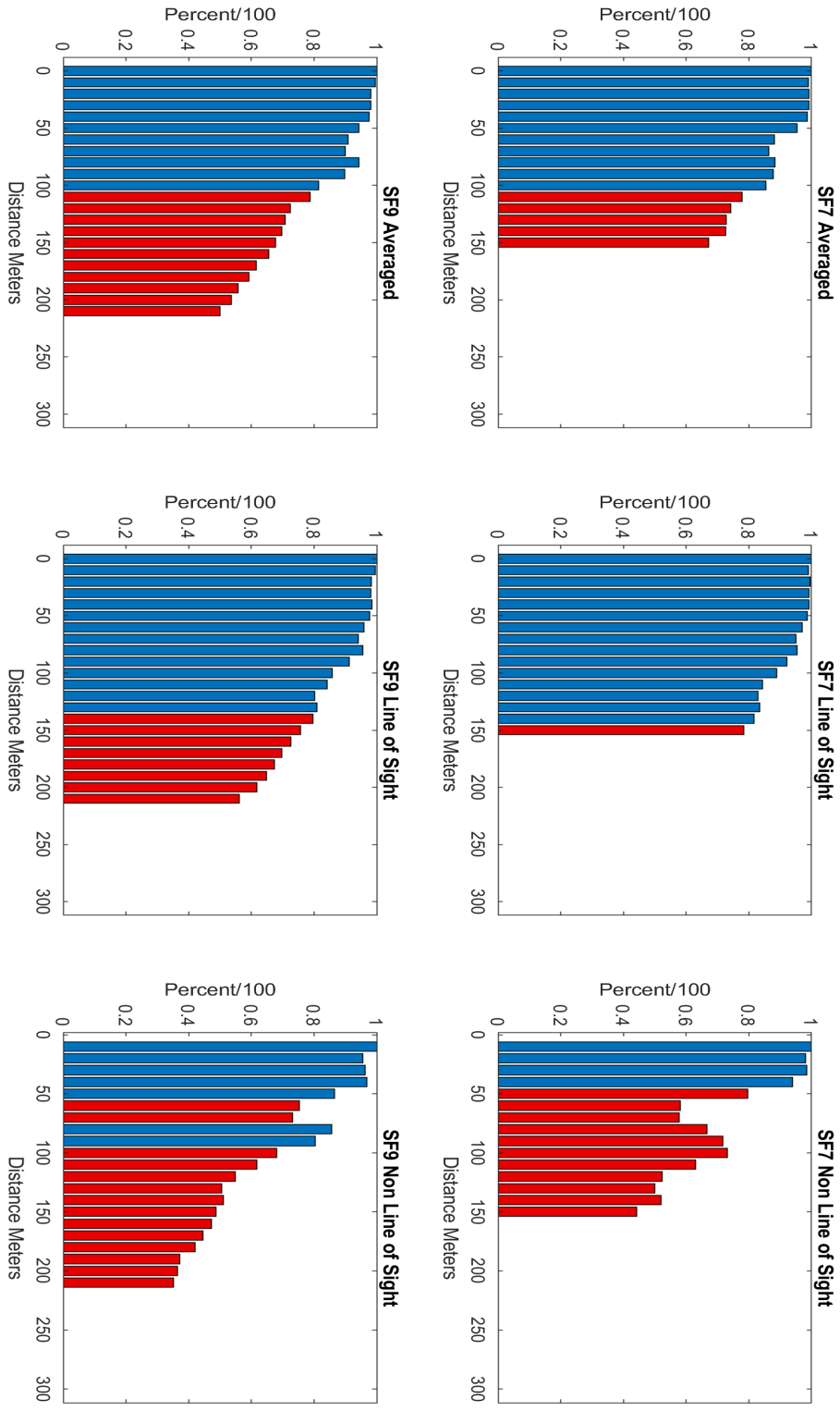

Figure 5.5: Gaussian averaged area outage rates

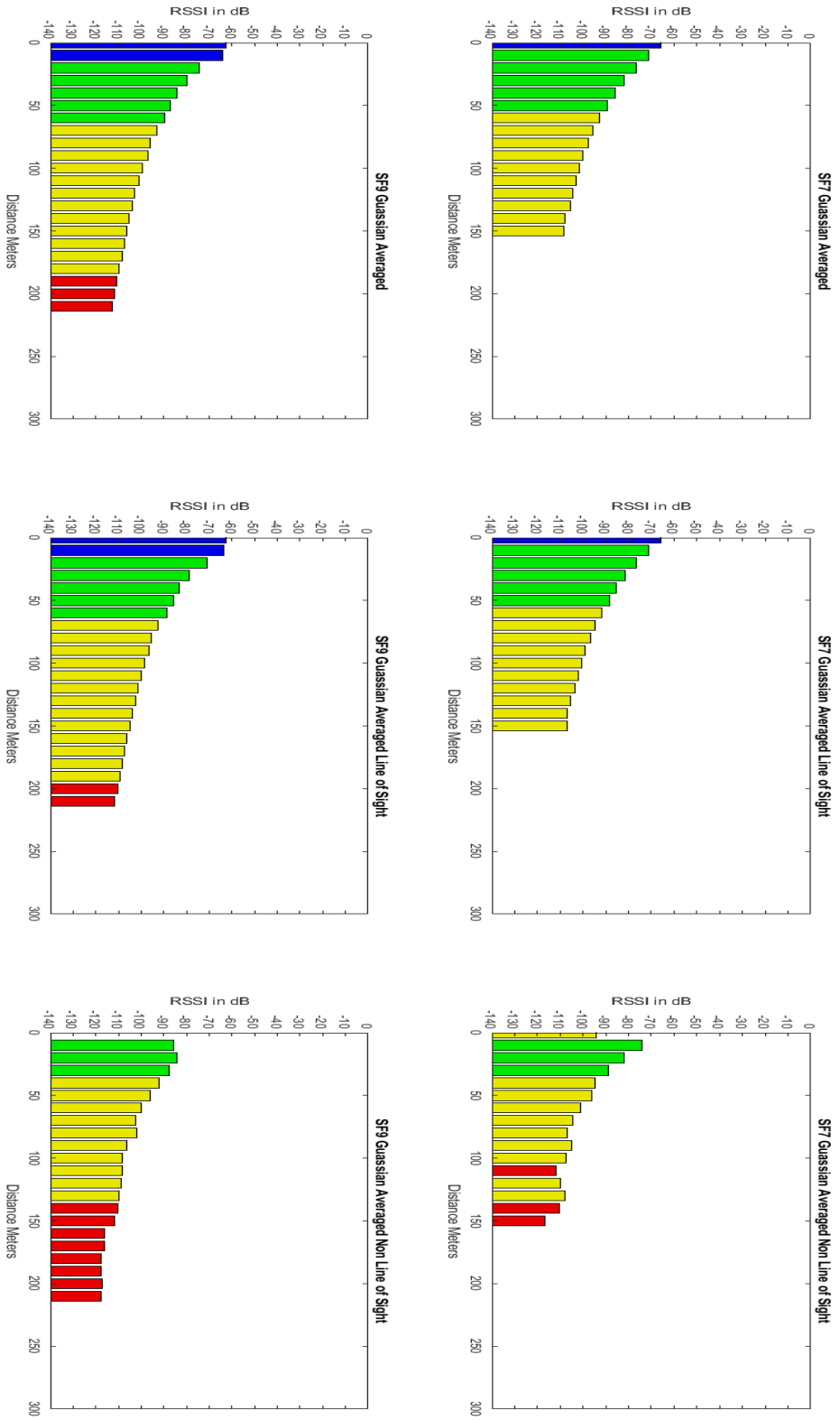

Figure 5.6: Gaussian averaged RSSI

5.1.2 Ground-level vs altitude

Most LoRa device deployment studies take place in more controlled environments with considerably more stable conditions which take into account factors like elevated antenna placement [42], LoS paths and static nodes to improve the testing environment. This makes link budget calculations, with a modified path-loss exponent, sufficient to predict approximate the behavior of inter-node connectivity.
But since this study is aimed at outdoor urban grounded applications (≈1.5 meters above ground), the propagation loss calculations may need to factor in losses from ground and buildings reflection components along with the landscape adding Fresnel zone attenuation described in2.6.2.2 which becomes significant with more than 40% blockage and makes LOS assumptions untenable at 55% [43][31]. While outside the scope of the testing, placing repeater nodes at a slightly higher altitude may provide clearance from Fresnel obstacles to providing higher transmission reliability across longer distances than what was obtained during range testing. Additionally, the ground-level placement also means an increase of people and vehicular traffic along with other obstacles that are not normally a large concern at altitude. This results in an increased impact by shadowing losses.

5.1.3 Area connectivity and scenario testing performance conclusions

When conducting spatial connectivity tests, it was assumed that the P2P wireless links had channel reciprocity, meaning that, if a node can receive a packet from a gateway, then the connection was considered to be near identical for the other way around as well [44]. The physical urban environment can impose location-specific wave propagation constraints in the form of deep shadowing fade and multi-path effects which may lead signals to face a slightly harsher RF channel traveling forth than back or vice-versa. The supporting data was found by comparing the received power levels at the gateway versus at the network nodes during scenario testing where RSSI values sometimes varied considerably between the two nodes' pings such as in the case of Alley 220 to Road LOS, seen in table 4.1, where a node in an alley space is pinging a road node 220 meters away in LOS conditions, but the RSSI variance between alley-to-road packets and road-to-alley ones was about 30 dB despite the high packet success rate of ≈ 97%.
It is worth noting that nodes in alleys were the most challenging to ping when a strong LoS component was not available in scenario tests, indicating the significance of empirical field testing as opposed to relying solely on the statistical predictive models. The discrepancies in link strength metrics across the different location categories highlight the importance of channel modeling. It takes into account the average signal power received along with RSSI variance data collected by conducting individual P2P link tests for the respective sites to obtain a more accurate assessment of the expected QoS from network nodes in those locations.
Relying on the effective range, area connectivity, site-specific tests, and the analysis conducted in the central Gothenburg location using the LoPy-s, an understanding of the possible QoS for sensor applications that can be provided was developed.

On average, a range of 100m per node hop employing SFs 7,9, and 11 could be reached with at least 80% packet success rate between nodes provided an LoS path is presented using only ground-level nodes. Thus, utilizing node-hopping, altitude and smart node-placement, it can be concluded that this methodology of mesh sensor network deployment can be used efficiently to operate monitoring applications that do not require large scale data per node. With more complex routing and mesh protocols to sustain higher node scalability, such networks could easily expand to cover down-town Gothenburg using only a small number of low-cost nodes. This demonstrates the edge that LoRa technology embedded devices have as a candidate to host smart city IoT applications while also their deployable limits.

5.1.4 Path loss model development

The models appear reasonable when compared to the scenario testing data. Given that they are both based on a theoretical base adjusted with empirical data, this is to be expected. A majority of the Average RSSI values fall within the probability distributions from the model. However, one aspect that was seen when looking at the pictures of the data sets was that the direct distance is not a good estimator for signal strength for the non-LoS which is supported by the larger distributions in the non-LoS models. This shows that signals are being reflected with a significant amount of power being preserved. Instead, what appears to be a more viable approach is something akin to a ray tracing approach, particularly in regards to closed spaces. Despite this, the model is still a good starting point in order to understand how unstable the RF path loss is in the urban space for LoRa.

5.2 Network design considerations

The custom network architecture was **tree-structured partial mesh** where sensor-nodes connected through hops to the gateway to abide by the different restrictions stemming from hardware limitations and transmitting on the wireless medium.
Looking at the requirements set in the introduction phase of the network design in section 1.4.2, the demo custom mesh network created will be evaluated:

1. The network is robust against node failure by tracking the active network nodes in a list and rerouting the pathways (if necessary) before every broadcasting cycle. The network algorithms can handle node movements within network range by creating a dynamic hierarchy classified by hops away from the gateway.
2. Packet exchange is synchronized using random ALOHA by creating random time slots for the nodes and is directed through scheduled beacons.
3. A network capacity of more than 80 nodes per nano-gateway was achieved with 3 hops.
4. Node placement flexibility is a function of the network's topology requirement to neighbor at least one other network node, theoretically allowing first and second branch nodes, on average, 50 meters of movement within the network's connectivity range.

5. A maximum network coverage range of 300 meters could be achieved with ground-level relay nodes.
6. While energy consumption was a factor in designing the network, battery lifetime calculations were not made as possible power sources became outside the scope of the project.
7. The nano-gateway primarily monitors the mesh protocols functioning against faults like node failures/restarts in co-ordination with the network nodes.
8. Node provisioning was handled at the network server level while database storage and the visual presentation was implemented on a metrics analyzer platform called Grafana.
9. The decentralized nature of the mesh architecture allows for multiple data sinks which can be used to decrease network congestion and increase its tolerance for scalability and node density.
10. The nodes in the network abided by the duty cycle limitations for the utilized spectrum, 869.4 MHz, 10 %, restricting the respective node's time on air to 360 seconds per hour.
11. Adaptive data rate protocol was not implemented in the network since LoRa protocol offers low data throughputs of less than 10 kbps minimizing the importance for heavy processing and energy intensive adaptive rate scheme.
12. Interoperability with LoRaWAN networks was not achieved as a different network scheme, and hence, packet structures were utilized by the custom mesh network implementation.

The network design was constrained by the physical layer specifications like time on air and its effect on the expected packet round-trip time which is an indicator to help decide the suitable routing and mesh protocols in upper OSI layers to provide reliable network support for sensor node communication. Due to the **long time-on-air** for packets sent in SF '11', transmission can take up to 600 milliseconds for payloads of size 20 bytes, thus, acknowledgment service beyond the first hop was not implemented. For the same reason, **on-demand routing was not adopted** since it will increase generated network control traffic and by that, latency.

Another consideration was the **limited signal processing capabilities of the gateway** used, which could only receive LoRa signals with a certain SF while listening to a single channel at a time. Thus, with higher capability gateways, adaptive data rates schemes and dedicated channels can be implemented in the network layer which would allow for higher node scalability.

Understanding the use-case intended for such sensor networks where the priorities will mostly revolve around **reliable transmission and energy conservation**. To increase reliability, introducing **selective redundancy** in sub-networks which can help nodes in areas of low signal penetration rates. The low energy consumption requirement for embedded sensor nodes, along with the duty cycle restrictions on the under-GHz spectrum, suggest the use of mesh and routing protocols with low complexity and less frequent control traffic utilizing the long-range property of LoRa. Energy saving features have been implemented in the design through tunable sleep and broadcasting cycles depending on the intended application despite not focusing

on battery life expectancy calculations.

5.3 Node positioning

To compensate for the difficult environment for network operation, an educated node layout can be utilized to provide coverage for large scale (city size) LoRa mesh projects in areas of low signal penetration rates. Gateways placed in higher altitudes, for example, over streetlight posts, can provide a higher range for connectivity and better coverage. LoRa nodes with an LoS component to the gateway (did not undergo heavy shadowing fade) show promising performance for substantial ranges when compared to other wireless communication protocols like Bluetooth low energy and Zigbee etc. With better area categorization and more elaborate testing, the channel starts becoming less unpredictable for non-LoS behavior and shadowing effect margins can be more accurately estimated to find more favorable locations for node-setup.

5.4 Methodology and data viability

Another important aspect to note with this report and the data gathered is if the methodology and the data gathered as a result is robust enough to provide support to the conclusions made in the report. Starting with the methodology, the idea to gather data in a way that was done could have been improved but ultimately still has merit. Firstly, the GPS coordinates used a mobile phone which as can be seen in the maps, was severely inaccurate in certain situations, with coordinates drifting upwards of 10 meters in certain cases causing data points to have an inherent level of spatial uncertainty. It also became apparent as testing was done that the early model of the LoPy as a measure of instability to its operation, either resulting in signals that should be received disappearing, data logging becoming corrupted, or RSSI measurements being gathered beneath their measurement floor in addition to the numerous crashes that plagued data gathering. Had more advanced equipment been available this would have been mitigated somewhat and increased data reliability. Additionally, the method of pinging base stations from a moving node worked well particularly when considering the varied data that was gathered but this opened up the risk to channel reciprocity issues corrupting the data as mentioned earlier as well as syncing issues between the various nodes. Furthermore, while the amount of data gathered was significant, there are great concerns as to how time dependent the measurements are considering that each location only has one or maybe a handful of data points to characterize its behavior. Finally, as can be seen in the number of samples graph in 4.13, certain distance measurement data and the conclusions drawn from them are inherently crippled by the lack of samples taken. This is very apparent when looking at samples per distance per position basis as can be seen in the appendix. These issues on top of the hidden data problem that results from the data being hidden by failed messages as discussed in 3.5.2 mean that the methodology has several flaws. Ideally, the methodology should have been reworked to have a number of random locations in Göteborg in which a node would transmit

to a large number of base stations in various locations which would log data over a long period of time to gain a large number of samples at each location. This would have resulted in more robust data gathered even if there was a loss in the variety of locations spatially. Using a more mobile spectrum analyzer to more robustly measure the noise floor and to see in what ways the LoRa packets are corrupted in certain locations would also be very helpful.

5.5 Viability of LoRa mesh at Ground-level in urban environments

Two main notes could be drawn from observing the testing results. The first being; the demonstration of a custom LoRa mesh network in an outdoor environment with the nodes (6 in total) at hand was successful in its task to display the extended range of operation feature as compared to a star topology by using the mesh multi-hopping property as opposed to centralized network topologies whose architecture pushes for simpler end node operations. Despite the low number of packets recorded, the performance gain can still be seen when observing the outage rate of node number 3 in table 4.3 for the custom mesh network vs when in LoRaWAN. While the packet success rate variation in nodes number 4 as seen in the second test in table 4.4, demonstrates the advantage of mesh routing in finding a signal path to the gateway in an environment challenged by obstacles and difficulty to achieve LoS to a node located in the alley.

The other note to take notice of was that the model created to predict the channel effects on the LoRa signal attenuation in urban Gothenburg was insufficient in certain scenarios. When LoS was provided, it was found that node performance could be predicted with more reliability up to certain distances. For SF '9', a communication distance of 140 meters could be achieved between nodes with 80% packet success rate given that LoS was available. These results from LoS connectivity test were a close match to the range testing limits that were conducted at earlier stages confirming the approach used in the methodology.
Also, P2P link tests at possible deployment locations along with altitude to ground coverage tests should be conducted which requires more man-power and a larger time frame than what was available to tackle channel reciprocity which is an important aspect of network connectivity. The generality of the model is yet to be experimented, meaning that, it is difficult to estimate how well the model may predict the system performance in a location with a different geographical topology than central Goteborg.

6
Future work

The analysis of urban LoRa mesh deployment metrics and assessing the testing methodology has provided some insights on some of the improvements that can be applied to the study in the future to obtain a deeper understanding of the urban channel behavior and its effect on the network.

6.1 Further data gathering

- Most tests were conducted during favorable weather conditions, a temperature of approximately 15 degrees with no rain. To have a more reliable data sample, an added number of tests can be performed during different times of the day to monitor the impact of urban traffic on the signal attenuation during various weather conditions. With the proper resource allocation, spatial connectivity and range tests can be expanded across more locations by moving the base station in smaller margins between the tests to obtain more stable and representative data samples.

- The use of a spectrum analyzer for outdoor measurements can help to obtain signal power readings (some LoRa transmissions were captured at an SNR of -11 dB at -125 dB) as they have higher sensitivity capabilities than the used embedded devices.

- P2P link performance tests for the respective possible deployment locations improves the channel model accuracy. Such tests were not conducted due to the time frame and resource limitations.

- Altitude range tests using LoRa has been done in numerous studies already and referred to in earlier works. But to get a better understanding of altitude coverage in dense urban locations under heavy shadowing, more tests need to be conducted. Rooftops and streetlights are suggestions of favorable locations for gateways to provide stronger coverage.

6.2 Simulation and modeling using data

When it comes to network deployments research in outdoor environment, it is a difficult and extensive task to create real-world testing scenarios and demos. Thus, software tools are used to simulate real-world channel conditions with proximity to

diagnose and test the network's different metrics with an increased scalability of nodes. Simulators like NS2 or OMNeT++ also give the option to test the effects of implementing different topologies, the efficiency of chosen network protocols and to track design faults and security bugs inherent in the system. Emulators and code level simulators like Avrora or ATEMU [45] can be more tailored for the use in wireless networks consisting of embedded device nodes.

6.3 Area study and positioning factors

Dedicated altitude tests to study the effect of eliminating Fresnel attenuation on LoRa signals in the urban location need to be conducted to be able to have a more realistic model of the possible signal behavior under shadowing. This will open the door for facilitating more network coverage by employing smart gateway placement a top of streetlight posts, wall mounting repeater nodes and using building rooftops etc. With regards to environment study, accurately defining LoS and non-LoS conditions with geographical characteristics like hills or frequent heavy traffic needs to be taken into consideration as that can affect the data analysis results in specific locations. Also, more solid guidelines for the categorization to describe the general physical environment to have a more general representation of the geographical RF effects of the urban environment in Sweden. For example, using official construction permit rules and regulations for central Gothenburg area to accurately quantify building sizes and density rather than relying on maps.

6.4 Network design and deployment

With a defined use-case, the mesh network features can be more tailored to include channel sensing to cover for crosstalk interference to sustain scalability. Using dedicated higher capability gateways like 'the things outdoor gateway' which can support up to 8 bands can allow for higher node capacity without sacrificing QoS by using smart algorithms like adaptive data rates to maintain a certain SINR threshold on different channels. When considering a private network deployment concerns of physical and application security need to be discussed by measuring the vulnerabilities of the system in terms of safety of the equipment as well as possible software threats from third parties like a Denial of Service 'DoS' or man in the middle attacks potentially risking the integrity and the functioning of the network.

6.5 Possible use cases

This thesis tends to explore the viability of LoRa mesh networks in urban outdoor deployments where sensor nodes are placed at ground-level in cases such as smart park meters, pollutant monitoring and service resource assignment although not exclusive to urban deployments. LoRa mesh can also fulfill the requirements of private networks installed in factory or indoor settings as the protocol's range can provide the connectivity support needed by the network nodes. LoRaWAN is currently being

deployed in numerous locations for asset tracking, logistics and smart monitoring, but a robust mesh network approach employing LoRa modulation may prove more economical, efficient and solution tailored especially for large-scale applications that span over cities to interconnect different sub-networks under common platforms. These advantages can be even more prevalent in open area applications like disaster warning and smart agriculture.

7
Conclusion

The project 's purpose revolved around creating a demonstration of a low power sensor network using Pycom embedded nodes and studying the feasibility of an outdoor urban set-up focusing on utilizing the LoRa long-range property in a mesh network topology A demonstration of the system was created successfully and tested in different areas, under different conditions, but due to lack of sufficient testing data, dedicated gateways and the need for simulation work to testify for the network nodes density scaling effects, the conclusion for the study of deploying a LoRa mesh sensor network in outdoor central Gothenburg was deemed inconclusive. But the various testing and analysis of the LoPy nodes' operation at the ground-level proved of great benefit not only due to the unprecedented nature of the deployment tested in that environment, but also for the insights provided on the shadowing and Fresnel loss as one of the main deterrents for the efficient functioning of such networks as seen through the variance of in the expected versus achieved range of connectivity, from a goal of around kilometer in favorable conditions (altitude, LoS, etc.) to an achievable range of less than 200 meters in ground-level set-ups. Despite that, the demonstration was able to present the advantageous features of applying the mesh principle, or at least partial in this case, to solidify the usability of the system in outdoor scenarios by allowing routing processes to take place at node level decreasing the need for dedicated gateways for small sub-networks, adding redundancy options for reliability and expanding connectivity range at the cost of security and power sacrifices. The potential of LoRa technology applied in mesh architecture as a candidate for IoT smart city applications was displayed by properties like superior range to competing communication protocols, robustness to interference and multipath, as well as ease of operation and cost-effective deployment.
More P2P link tests need to be conducted while adopting a stricter area division scheme in order to generalize the models developed over larger urban locations. Also, testing the heterogeneous effect of adding relay gateways placed at a higher altitude like streetlights and wall mounting on coverage expansion by providing stronger LoS pathways to the nodes and reducing signal propagation losses.

Bibliography

[1] M. J. Feuerstein, K. L. Blackard, T. S. Rappaport, S. Y. Seidel, and H. H. Xia, "Path loss, delay spread, and outage models as functions of antenna height for microcellular system design," *IEEE Transactions on Vehicular Technology*, vol. 43, no. 3, pp. 487–498, 1994.

[2] K. Staniec and M. Kowal, "Lora performance under variable interference and heavy-multipath conditions," *Wireless Communications and Mobile Computing*, vol. 2018, pp. 1–9, 04 2018.

[3] A. R. F. B. Christian Ebi, Fabian Schaltegger, "Synchronous lora mesh network to monitor processes in underground infrastructure," *IEEE ACCESS*, vol. 7, pp. 57 663 – 57 677, 04 2019. [Online]. Available: https://www.researchgate.net/publication/332773089_Synchronous_LoRa_Mesh_Network_to_Monitor_Processes_in_Underground_Infrastructure

[4] H. C. W. Lee and K.-H. Ke, "Monitoring of large-area iot sensors using a lora wireless mesh network system: Design and evaluation," *IEEE Transactions on Instrumentation and Measurement*, vol. 67, pp. 2177–2187, 03 2018. [Online]. Available: https://ieeexplore.ieee.org/document/8326735

[5] D. L. A. H. C. N. E. Fitzgerald, "A routing protocol for lora mesh networks," 06 2018. [Online]. Available: https://ieeexplore.ieee.org/document/8449743

[6] J. M. Hechmi, A. Zrelli, M. Kbida, H. Khlaifi, and T. Ezzedine, "Coverage and connectivity of wsn models for health open-pit mines monitoring," in *2018 14th International Wireless Communications Mobile Computing Conference (IWCMC)*, 2018, pp. 310–315.

[7] S. Bai and J. Jiao, "Dockless e-scooter usage patterns and urban built environments: A comparison study of austin, tx, and minneapolis, mn," *Travel Behaviour and Society*, vol. 20, pp. 264–272, 04 2020.

[8] T. Al-Wajeeh, "Efficient radio channel modeling for urban wireless sensors networks," 2018. [Online]. Available: https://tel.archives-ouvertes.fr/tel-02864456

[9] S. M. Mohamed, H. S. Hamza, and I. A. Saroit, "Coverage in mobile wireless sensor networks (m-wsn): A survey," *Computer Communications*, vol. 110, pp. 133 – 150, 2017. [Online]. Available: http://www.sciencedirect.com/science/article/pii/S0140366417307235

[10] Pycom, "Pycom documentation," Available at https://docs.pycom.io/ (2020/06/23).

[11] ——, "Pycom antenna," Available at https://pycom.io/product/lora-868mhz-915mhz-sigfox-antenna-kit/ (2020/06/23).

[12] Ettus, "Usrp hardware driver and usrp manual," Available at https://files.ettus.com/manual/page_usrp2.html (2020/06/23).

[13] Microsoft, "Visual studio code 2019," Available at https://code.visualstudio.com (2020/06/23).

[14] D. George, "Micropython," Available at https://micropython.org/ (2020/06/23).

[15] Mathworks, "Matlab," Available at https://www.mathworks.com/products/matlab.html (2020/06/23).

[16] I. F. Akyildiz, X. Wang, and W. Wang, "Wireless mesh networks: a survey," *Computer Networks*, vol. 47, no. 4, pp. 445 – 487, 2005. [Online]. Available: http://www.sciencedirect.com/science/article/pii/S1389128604003457

[17] C. Zhu, C. Zheng, L. Shu, and G. Han, "A survey on coverage and connectivity issues in wireless sensor networks," *Journal of Network and Computer Applications*, vol. 35, no. 2, pp. 619 – 632, 2012, simulation and Testbeds. [Online]. Available: http://www.sciencedirect.com/science/article/pii/S1084804511002323

[18] S. Meguerdichian, F. Koushanfar, M. Potkonjak, and M. B. Srivastava, "Coverage problems in wireless ad-hoc sensor networks," in *Proceedings IEEE INFOCOM 2001. Conference on Computer Communications. Twentieth Annual Joint Conference of the IEEE Computer and Communications Society (Cat. No.01CH37213)*, vol. 3, 2001, pp. 1380–1387 vol.3.

[19] DavidJ.C.MacKay, *Information Theory, Inference, and Learning Algorithms*, 2005. [Online]. Available: https://www.inference.org.uk/itprnn/book.pdf

[20] A. Leon-Garcia and I. Widjaja, *Communication Networks: Fundamental Concepts and Key Architectures*, ser. Computer Science Series. McGraw-Hill, 2000. [Online]. Available: https://books.google.se/books?id=BQ4fAQAAIAAJ

[21] L. Alliance, "Lorawan regional parameters specification," Available at https://lora-alliance.org/sites/default/files/2020-01/rp2-1.0.0_final_release.pdf (2020/06/23), 2018.

[22] Semtech, "Lora modulation basics," Available at https://semtech.my.salesforce.com/sfc/p/#E0000000JelG/a/2R0000001OJu\/xvKUc5w9yjG1q5Pb2IIkpolW54YYqGb.frOZ7HQBcRc (2020/06/23).

[23] ——, "Implementing data whitening and crc calculation in software on sx12xx devices," Available at https://semtech.my.salesforce.com/sfc/p/#E0000000JelG/a/2R000000HSP2/oLQW1WLmWO5HB4S_vdzDX_wIB5ykObyTgp16Cz9ceoQ (2020/06/23), Tech. Rep.

[24] M. Chiani and A. Elzanaty, "On the lora modulation for iot: Waveform properties and spectral analysis," *IEEE Internet of Things Journal*, 2019.

[25] Semtech, "cities get smarter with lora technlogy," Available at https://blog.semtech.com/cities-get-smarter-with-lora-technology (2020/10/31).

[26] lora alliance, "What is the lorawan® specification?" Available at https://lora-alliance.org/about-lorawan (2020/10/30).

[27] in *Probability and Random Processes (Second Edition)*, second edition ed., S. L. Miller and D. Childers, Eds. Boston: Academic Press, 2012. [Online]. Available: http://www.sciencedirect.com/science/article/pii/B9780123869814500023

[28] "Tätorter; arealer, befolkning 2010," 2010.

[29] M. A. Marsan, G. C. Hess, and S. Gilbert, "Shadowing variability in an urban land mobile environment at 900 mhz," 1990.

[30] A. Goldsmith, *Wireless Communications*. Cambridge University Press, 2013. [Online]. Available: https://books.google.se/books?id=ZtFVAgAAQBAJ

[31] T. Rappaport, *Wireless Communications: Principles and Practice*, ser. Electrical engineering. Prentice Hall PTR, 1996. [Online]. Available: https://books.google.se/books?id=C_pSAAAAMAAJ

[32] B. Dhoedt and J. Hoebeke, "An overview of mobile ad hoc networks: Applications and challenges," *Communication network journal*, 2004.

[33] S. Misra, S. Misra, and I. Woungang, *Guide to Wireless Mesh Networks*, 01 2009.

[34] S. A. Mahmud, S. Khan, S. Khan, and H. Al-Raweshidy, "A comparison of manets and wmns: Commercial feasibility of community wireless networks and manets," 2006.

[35] S. Pervez, "Wireless mesh network architecture and applications," April 2016.

[36] S. Puri and V. Arora, "Routing protocols in manet: A survey," *International Journal of Computer Applications*, vol. 96, no. 13, pp. 7–12, 2014. [Online]. Available: https://www.researchgate.net/publication/271156613_Routing_Protocols_in_MANET_A_Survey

[37] G. G. Andreadis, Alessandro, *Protocols for High-Efficiency Wireless Networks*. Springer US, 2002. [Online]. Available: https://www.springer.com/gp/book/9781402073267?utm_campaign=bookpage_about_buyonpublisherssite&utm_medium=referral&utm_source=springerlink

[38] C. E. C. Committee, "Erc recommendation 70-03 relating to the use of short range devices (srd)," Tech. Rep., 2020. [Online]. Available: https://www.ecodocdb.dk/download/25c41779-cd6e/Rec7003e.pdf

[39] Pycom, "Lopy," 2018. [Online]. Available: https://pycom.io/wp-content/uploads/2018/08/lopy-specsheet.pdf

[40] C. F. A. F. B. G. B. H. J. K. Peter von Butovitsch, David Astely and E. Larsson, "Advanced antenna systems for 5g networks," 11 2018.

[41] P. K. Sharma and . R. Singh, "A modified approach to calculate the path loss in urban area," *International Journal of Electronics and Communication Engineering*, vol. 4, no. 4, pp. 453–460, 2011. [Online]. Available: https://www.ripublication.com/irph/ijece/ijecev4n4___10.pdf

[42] A. Torabi, "Channel modeling for fifth generation cellular networks and wireless sensor networks," 2016. [Online]. Available: https://core.ac.uk/download/pdf/151509122.pdf

[43] H. Bertoni and S. Torrico, "Chapter 6 - properties and measures of the radio channel," in *Academic Press Library in Mobile and Wireless Communications*, S. K. Wilson, S. Wilson, and E. Biglieri, Eds. Oxford: Academic Press, 2016, pp. 193 – 225. [Online]. Available: http://www.sciencedirect.com/science/article/pii/B9780123982810000065

[44] R. Wilson, D. Tse, and R. A. Scholtz, "Channel identification: Secret sharing using reciprocity in ultrawideband channels," *IEEE Transactions on Information Forensics and Security*, vol. 2, no. 3, pp. 364–375, 2007.

[45] B. Musznicki and P. Zwierzykowski, "Survey of simulators for wireless sensor networks," 09 2012. [Online]. Available: https://www.researchgate.net/publication/234065225_Survey_of_Simulators_for_Wireless_Sensor_Networks

A

Appendix 1

The below table presents the full results of the P2P scenario tests conducted by showing the packet success rate and RSSI average and variance values, from which a sample was captured in table 4.1.

Location_Distance_Location_Sight	Outage Rate	Average RSSI	RSSI Variance
Alley_53_Alley_LOS	0.938	-94.938	47.076
Alley_53_Alley_NLOS	0.923	-109.603	17.605
Alley_53_Open_LOS	1	-79.551	65.034
Alley_53_Open_NLOS	0.958	-95.113	51.350
Alley_53_Road_LOS	0.979	-88.523	26.487
Alley_53_Road_NLOS	0.957	-110.910	9.356
Alley_106_Alley_LOS	0.968	-98.103	19.989
Alley_106_Alley_NLOS	0	-122	0
Alley_106_Open_LOS	0.946	-105.858	27.867
Alley_106_Open_NLOS	0	-122	0
Alley_106_Road_LOS	0.990	-81.068	36.379
Alley_106_Road_NLOS	0.989	-105.802	18.752
Alley_160_Alley_LOS	0.967	-103.591	17.331
Alley_160_Alley_NLOS	0	-122	0
Alley_160_Open_LOS	0.989	-108.387	4.329
Alley_160_Open_NLOS	0	-122	0
Alley_160_Road_LOS	0.968	-90.548	50.011
Alley_160_Road_NLOS	0	-122	0
Open_53_Alley_LOS	1	-79.730	53.670
Open_53_Alley_NLOS	0.958	-95.815	47.032
Open_53_Open_LOS	0.979	-81.074	58.073
Open_53_Open_NLOS	0.012	-121.849	0.429
Open_53_Road_LOS	0.947	-105.369	24.731
Open_53_Road_NLOS	0.978	-89.177	35.304
Open_106_Alley_LOS	0.946	-105.602	25.851
Open_106_Alley_NLOS	0	-122	0
Open_106_Open_LOS	0.968	-88.929	55.605
Open_106_Open_NLOS	0.570	-112.698	32.822
Open_106_Road_LOS	0.957	-102.572	17.450
Open_106_Road_NLOS	0	-122	0
Open_160_Alley_LOS	0.989	-106.682	5.127
Open_160_Alley_NLOS	0	-122	0
Open_160_Open_LOS	0.968	-97.385	25.778
Open_160_Open_NLOS	0.244	-113.003	36.369
Open_160_Road_LOS	0.914	-105.901	31.149
Open_160_Road_NLOS	0.133	-120.664	3.777
Road_53_Alley_LOS	0.979	-88.323	26.882
Road_53_Alley_NLOS	0.957	-109.945	13.438
Road_53_Open_LOS	0.946	-103.822	30.189
Road_53_Open_NLOS	0.979	-91.245	31.065
Road_53_Road_LOS	0.787	-103.489	67.330
Road_53_Road_NLOS	0.868	-104.950	42.138
Road_106_Alley_LOS	0.990	-80.628	44.895
Road_106_Alley_NLOS	0.989	-109.685	12.392
Road_106_Open_LOS	0.957	-103.538	16.058
Road_106_Open_NLOS	0	-122	0
Road_106_Road_LOS	0.820	-108.977	31.072
Road_106_Road_NLOS	0.025	-121.211	2.234
Road_160_Alley_LOS	0.968	-91.132	60.599
Road_160_Alley_NLOS	0	-122	0